(12) LEVEL II

RADC-TR-79-26
Final Technical Report
March 1979

STATISTICS OF SPECKLE PROPAGATION

Oregon Graduate Center

Sponsored by
Defense Advanced Research Projects Agency (DoD)
ARPA Order No. 1279

The views and conclusions contained in this document are those of the authors and should not be interpreted as necessarily representing the official policies, either expressed or implied, of the Defense Advanced Research Projects Agency or the U.S. Government.

ROME AIR DEVELOPMENT CENTER
Air Force Systems Command
Griffiss Air Force Base, New York 13441

This report has been reviewed by the RADC Information Office (OI) and is releasable to the National Technical Information Service (NTIS). At NTIS it will be releasable to the general public, including foreign nations.

RADC-TR-79-26 has been reviewed and is approved for publication.

APPROVED: Robert F. Ogrodnik

ROBERT F. OGRODNIK
Project Engineer

If your address has changed or if you wish to be removed from the RADC mailing list, or if the addressee is no longer employed by your organization, please notify RADC (OCTM) Griffiss AFB NY 13441. This will assist us in maintaining a current mailing list.

Do not return this copy. Retain or destroy.

UNCLASSIFIED

SECURITY CLASSIFICATION OF THIS PAGE (When Data Entered)

REPORT DOCUMENTATION PAGE

READ INSTRUCTIONS BEFORE COMPLETING FORM

1. REPORT NUMBER: RADC-TR-79-261	2. GOVT ACCESSION NO.
3. RECIPIENT'S CATALOG NUMBER	
4. TITLE (and Subtitle): STATISTICS OF SPECKLE PROPAGATION	5. TYPE OF REPORT & PERIOD COVERED: Final Technical Report, 1 Jan 78 — 30 Sep 78
6. PERFORMING ORG. REPORT NUMBER: N/A	
7. AUTHOR(s): J. Richard Kerr, Myung H. Lee, Charles M. McIntyre, James H. Churnside	8. CONTRACT OR GRANT NUMBER(s): F30602-78-C-0064, ARPA Order-1279
9. PERFORMING ORGANIZATION NAME AND ADDRESS: Oregon Graduate Center, 19600 N. W. Walker Road, Beaverton OR 97005	10. PROGRAM ELEMENT, PROJECT, TASK AREA & WORK UNIT NUMBERS: 62301E, 12790028, 00
11. CONTROLLING OFFICE NAME AND ADDRESS: Defense Advanced Research Projects Agency, 1400 Wilson Blvd, Arlington VA 22209	12. REPORT DATE: March 1979
	13. NUMBER OF PAGES: 64
14. MONITORING AGENCY NAME & ADDRESS (if different from Controlling Office): Rome Air Development Center (OCTM), Griffiss AFB NY 13441	15. SECURITY CLASS. (of this report): UNCLASSIFIED
	15a. DECLASSIFICATION DOWNGRADING SCHEDULE: N/A

16. DISTRIBUTION STATEMENT (of this Report)

Approved for public release; distribution unlimited.

17. DISTRIBUTION STATEMENT (of the abstract entered in Block 20, if different from Report)

Same

18. SUPPLEMENTARY NOTES

RADC Project Engineer: Robert F. Ogrodnik (OCTM)

19. KEY WORDS (Continue on reverse side if necessary and identify by block number)

Propagation
Turbulence
Glint
Scintillation
Speckles

20. ABSTRACT (Continue on reverse side if necessary and identify by block number)

The study of the statistical effects of atmospheric turbulence on coherent radiation scattered from a diffuse target is extended, both theoretically and experimentally, to include the effects of target glint and partial temporal coherence of the source.

Theoretically, expressions are developed for 1st and 2nd order moments of irradiance for targets containing multiple glints, and for a partially coherent source. The expression for the normalized variance of irradiance for a diffuse target with a single glint illuminated by a coherent source over a (Cont'd)

DD FORM 1 JAN 73 1473 EDITION OF 1 NOV 65 IS OBSOLETE

UNCLASSIFIED

SECURITY CLASSIFICATION OF THIS PAGE (When Data Entered)

390 077

Item 20 (Cont'd)

horizontal atmospheric path is evaluated numerically for comparison with experimental results. Experimental measurements of the variance and covariance of irradiance for a coherent source illuminating a diffuse target containing a single glint are discussed along with preliminary results for the illumination of a diffuse target with a partially coherent source.

TABLE OF CONTENTS

		Page
I.	Introduction	1
II.	Theoretical Description	5
	A. Introduction	5
	B. Mutual Coherence Function and Mean Irradiance	6
	C. Covariance of Irradiance	17
	D. Speckle Patterns with Reduced Source Coherence	25
III.	Numerical Evaluation	31
IV.	Experimental Results	40
	A. Introduction	40
	B. Target Glint	41
	C. Partially Coherent Source	50
V.	Discussion	53
	References	55
	Appendix	A-1

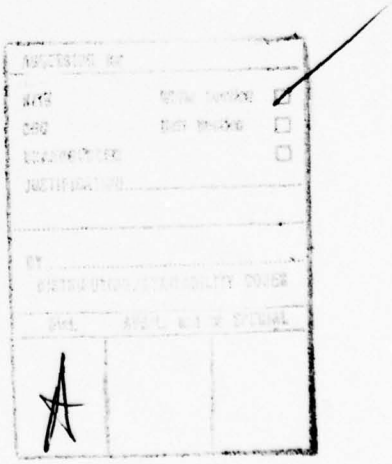

A036503

I. Introduction

This program is an extension of the work performed under contract F30602-74-C-0082 and reported in the Final Technical Report released in January 1977 (RADC-TR-77-18). A major contribution of that work was the exposition of a complete theory for the statistical effects of atmospheric turbulence on coherent radiation reflected from a diffuse target, including the effects of both phase and amplitude perturbations. In this report, we discuss an extension of the previous work utilizing the complete theory developed there and including a thorough experimental investigation.

The objective of the present work was to extend the previous results, both experimentally and theoretically, in two directions: one to evaluate the effect of target glint, and the other to consider the influence of source coherence. Both of these directions have led to significant results that will impact system considerations.

- With a single glint on an otherwise diffuse target we have found that the normalized variance of the scattered irradiance is enhanced over that from a diffuse target alone. This increased normalized variance (on the order of 3) corresponds to a substantial increase in the fluctuations of the received irradiance.
- With a small but finite source bandwidth, we have found that the normalized variance of the irradiance scattered from a diffuse target is unexpectedly decreased from that when a "coherent" source is used. This corresponds to a substantial decrease in the fluctuations of the received irradiance.

In addressing the issue of target glint, we were faced with the question of what to use as a glint in the experimental configuration, and what theoretical model should be used to represent this glint. The question arises because of both the experimental constraints imposed by the targets of interest and by the numerical evaluation of the complex theoretical expressions that accurately model the propagation geometry. The theoretical model chosen is discussed in Section IIA. Experimentally, we wanted to ensure that the irradiance received was not dominated by either the diffuse term or the coherent (glint) term alone, in order that the experimental results included a realm where both terms were effective in influencing the statistics of the received irradiance. Since the diffuse portion of the target scatters the incident radiation into large angles, the received irradiance due to the diffuse target is small. This required that the received irradiance due to the glint be small also, and consequently that the coherent feature on the target be small. We felt that a retro-reflector glint did not satisfactorily represent a real glint, and since the required radius of curvature of a curved specular surface that would give an appropriate level of irradiance at the target was extremely large, the experimental glint was chosen to be a small flat mirror. This was quite practical experimentally and gave results in good agreement with the theoretical model chosen.

In addressing the issue of source coherence, we utilized an Argon ion laser operating on the 488 nanometer line and contrasted the results with and without a temperature stabilized, intra-cavity etalon. With the etalon in place, the laser output consisted of a single longitudinal TEM_{oo} mode.

With the etalon removed, multiple longitudinal modes were allowed to run covering the full 488 nanometer linewidth. The linewidth is on the order of 10^{10} Hertz and this configuration reduced the coherence length to approximately 3 centimeters.

The basic experimental configuration is shown in Figure 1. The source is an Argon ion laser operating at 488 nanometers that can be conveniently modified to run either single or multimode. The propagation path is nominally 500 meters over flat featureless farm land. The receiver consists of two photomultiplier tubes, each with a 1 millimeter aperture. The spacing of the two apertures is variable to allow measurement of the spatial correlation function.

This report includes the results of a detailed theoretical investigation of speckle propagation in atmospheric turbulence using the extended Huygens Fresnel principle. This investigation is set forth in Section II. The numerical evaluation of particular theoretical expressions is discussed in Section III. The experimental program is described in Section IV and exprimental results are presented and compared with the numerical results where appropriate. A discussion of the results in Section V concludes the report.

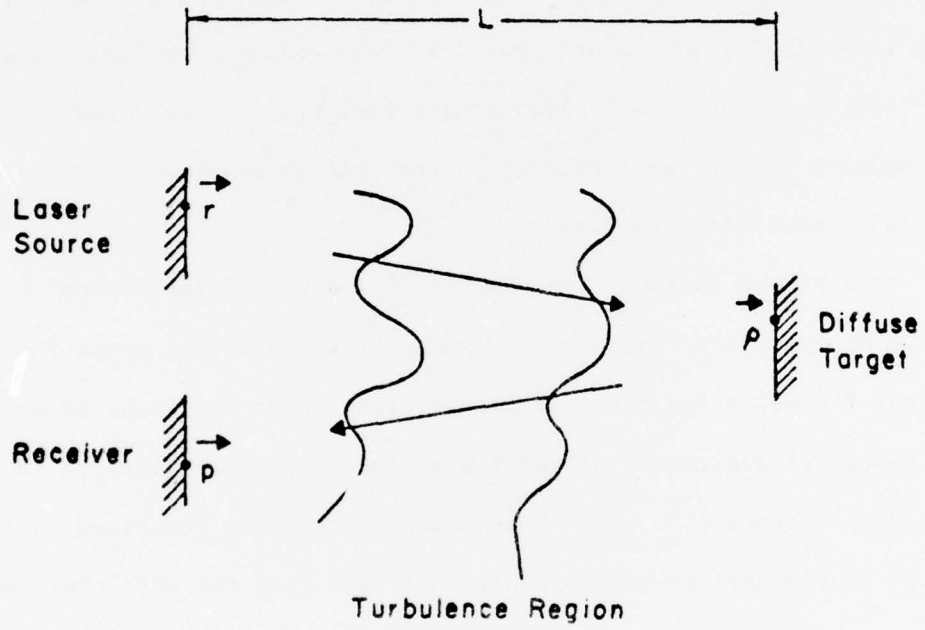

Figure 1. Illuminator, Target and Receiver Configuration

II. Theoretical Description

A. Introduction

Theoretically, we are interested in describing the statistical nature[1,2,3] of the field scattered from a target in the geometry shown schematically in Figure 1. In order to do this, we use the extended Huygens Fresnel[4,5] principle to compute the field incident on the target due to a focused gaussian beam propagating over an atmospherically turbulent path. The field scattered from the target is then related to the incident field using the known characteristics of the target. Finally this scattered field is propagated back to the receiver using the extended Huygens Fresnel principle once again. This gives an expression for the field at the receiver that may be used to compute the statistical averages of interest. In this Section we compute the mean irradiance for a coherent source and a diffuse target with multiple glints in part B. In part C we evaluate the second order moments, namely variance and covariance of irradiance. The results of part B are then extended to include reduced source coherence in part D.

B. Mutual Coherence Function and Mean Irradiance

With $\vec{r}$ denoting a two-dimensional coordinate vector in the plane of the transmitter aperture, the source amplitude distribution for a single mode laser transmitter is

$$U_o(\vec{r}) = U_o \exp\left(-\frac{r^2}{2\alpha_o^2} - \frac{ik}{2F} r^2\right) \tag{1}$$

where $r = |\vec{r}|$,

α_o = the radius where the intensity is e^{-1} of the intensity at $r = 0$,

$k = \frac{2\pi}{\lambda}$,

λ = wavelength, and

F = the focal length.

Using the extended Huygens Fresnel principle, the field at the target can be expressed

$$U_i(\vec{\rho}) = \frac{k}{2\pi iL} \exp(ikL) \int U_o(\vec{r}) \exp\left[\frac{ik|\vec{\rho} - \vec{r}|^2}{2L} + \psi_1(\vec{\rho}, \vec{r})\right] d\vec{r} \tag{2}$$

where $U_i(\vec{\rho})$ = the field incident upon the target,

$\vec{\rho}$ = a two-dimensional coordinate vector in the plane of the target,

L = path length,

and $\psi_1(\vec{\rho}, \vec{r})$ describes the effects of the random medium (atmospheric turbulence) on the propagation of a spherical wave from the source to the target.

For a target composed of a diffuse surface containing multiple glints, the field scattered from the target can be written

$$U_s(\vec{\rho}) = U_d(\vec{\rho}) + U_g(\vec{\rho}) \tag{3}$$

where $U_d(\vec{\rho})$ is that portion of the scattered field due to the diffuse surface, and $U_g(\vec{\rho})$ is that portion of the scattered field due to the multiple glints. The field scattered from the diffuse portion of the target can be written[6]

$$U_d(\vec{\rho}) = -R^{1/2}\, U_i(\vec{\rho}) \tag{4}$$

where R is the reflectivity of the diffuse surface. Assuming that a cube corner is a valid model for a small glint, the field reflected from the multiple glints may be written[7]

$$U_g(\vec{\rho}) = \sum_{m=1}^{M} a_m\, r_m(\vec{\rho})\, U_i^*(\vec{\rho}_m) \tag{5}$$

where a_m = the complex strength of the m^{th} glint,

$r_m(\vec{\rho})$ = the effective amplitude reflection coefficient of the m^{th} glint, and

$\vec{\rho}_m$ = the position of the m^{th} glint, and

M = the number of glints.

In the following development, we will assume that for small glints, $r_m(\vec{\rho})$ has a gaussian form, i.e.

$$r_m(\vec{\rho}) = \exp\left(-\frac{|\vec{\rho} - \vec{\rho}_m|^2}{(\Delta\rho_m)^2}\right) \tag{6}$$

where $\Delta\rho_m$ = the "width" of the m^{th} glint.

In terms of the field scattered from the target, the field at the receiver may be obtained by reapplying the extended Huygens Fresnel principle. Thus

$$U_r(\vec{p}) = \frac{k}{2\pi iL} \exp(ikL) \int U_s(\vec{\rho}) \exp\left[\frac{ik|\vec{p} - \vec{\rho}|^2}{2L} + \psi_2(\vec{p}, \vec{\rho})\right] d\vec{\rho} \quad (7)$$

where $U_r(\vec{p})$ = the field at the receiver,

$\vec{p}$ = a two-dimensional coordinate vector in the plane of the receiver,

and $\psi_2(\vec{p}, \vec{\rho})$ describes the effect of atmospheric turbulence on the propagation of a spherical wave from the target to the receiver.

At this point, we can write an expression for the mutual coherence function, $\Gamma(\vec{p}_1, \vec{p}_2)$.

$$\begin{aligned}\Gamma(\vec{p}_1, \vec{p}_2) &= \langle U_r(\vec{p}_1)\, U_r^*(\vec{p}_2)\rangle \\ &= \left(\frac{k}{2\pi L}\right)^2 \iint d\vec{\rho}_1 d\vec{\rho}_2 \langle U_s(\vec{\rho}_1)\, U_s^*(\vec{\rho}_2)\rangle \\ &\quad \times \exp\left[\frac{ik|\vec{p}_1 - \vec{\rho}_2|^2}{2L} - \frac{ik|\vec{p}_2 - \vec{\rho}_2|^2}{2L}\right] \\ &\quad \times \langle \exp\left[\psi_2(\vec{p}_1, \vec{\rho}_1) + \psi_2^*(\vec{p}_2, \vec{\rho}_2)\right]\rangle \end{aligned} \quad (8)$$

where the * indicates the complex conjugate and the angular brackets < > indicate ensemble averaging. The mutual coherence function of the scattered field contained in the integrand of equation (8) can be rewritten

$$\langle U_s(\vec{\rho}_1)\, U_s^*(\vec{\rho}_2)\rangle = \langle \left[U_d(\vec{\rho}_1) + U_g(\vec{\rho}_1)\right]\left[U_d(\vec{\rho}_2) + U_g(\vec{\rho}_2)\right]^*\rangle$$

$$= \langle U_d(\vec{\rho}_1)\ U_d^*(\vec{\rho}_2)\rangle + \langle U_d(\vec{\rho}_1)\ U_g^*(\vec{\rho}_2)\rangle$$

$$+ \langle U_g(\vec{\rho}_1)\ U_d^*(\vec{\rho}_2)\rangle + \langle U_g(\vec{\rho}_1)\ U_g^*(\vec{\rho}_2)\rangle \qquad (9)$$

The diffusely reflected fields are spatially incoherent so that

$$\langle U_d(\vec{\rho}_1)\ U_d^*(\vec{\rho}_2)\rangle = \frac{4\pi}{k^2} \langle I_d(\vec{\rho}_1)\rangle\ \delta(\vec{\rho}_1 - \vec{\rho}_2) \qquad (10)$$

where $\langle I_d(\vec{\rho}_1)\rangle = \langle U_d(\vec{\rho}_1)\ U_d^*(\rho_1)\rangle$, and $\delta(\vec{\rho}_1 - \vec{\rho}_2)$ is the Dirac delta function. Also, due to the spatial incoherence of the diffusely reflected fields,

$$\langle U_d(\vec{\rho}_1)\ U_g^*(\vec{\rho}_2)\rangle = \langle U_g(\vec{\rho}_1)\ U_d^*(\vec{\rho}_2)\rangle = 0 \qquad (11)$$

Then

$$\langle U_s(\vec{\rho}_1)\ U_s^*(\vec{\rho}_2)\rangle = \frac{4\pi R}{k^2} \langle I_i(\vec{\rho}_1)\rangle\ \delta(\vec{\rho}_1 - \vec{\rho}_2)$$

$$+ \sum_{m_1 = 1}^{M} \sum_{m_2 = 1}^{M} a_{m_1}\ a_{m_2}^*\ \langle U_i^*(\vec{\rho}_{m_1})\ U_i(\vec{\rho}_{m_2})\rangle$$

$$\times \exp\left[- \frac{|\vec{\rho}_1 - \vec{\rho}_{m_1}|^2}{(\Delta\rho_{m_1})^2} - \frac{|\vec{\rho}_2 - \vec{\rho}_{m_2}|^2}{(\Delta\rho_{m_2})^2} \right] \qquad (12)$$

Following this we will assume that the glints are identical, i.e. that $a_{m_i} = 1$ and $\Delta\rho_{m_i} = \Delta\rho_w$.

Since from equation (11), the cross correlation terms are zero, the mutual coherence function of equation (8) can be expressed as the sum of a diffuse component and a "specular" component (from the multiple glints):

$$\Gamma(\vec{p}_1, \vec{p}_2) = \Gamma_d(\vec{p}_1, \vec{p}_2) + \Gamma_g(\vec{p}_1, \vec{p}_2). \tag{13}$$

From equations (8) and (12),

$$\Gamma_d(\vec{p}_1, \vec{p}_2) = \frac{R}{\pi L^2} \iint d\vec{\rho}_1 d\vec{\rho}_2 \, \langle I_i(\vec{\rho}_1)\rangle \, \delta(\vec{\rho}_1 - \vec{\rho}_2) \times \exp\left[\frac{ik|\vec{p}_1 - \vec{\rho}_1|^2}{2L} - \frac{ik|\vec{p}_2 - \vec{\rho}_2|^2}{2L}\right] \times \langle \exp[\psi_2(\vec{p}_1, \vec{\rho}_1) + \psi_2^*(\vec{p}_2, \vec{\rho}_2)]\rangle \tag{14}$$

The delta function allows us to perform one integration, and using

$|\vec{p}_j - \vec{\rho}_j|^2 = (\vec{p}_j - \vec{\rho}_j) \cdot (\vec{p}_j - \vec{\rho}_j)$, and

$$\langle \exp[\psi_2(\vec{p}_1, \vec{\rho}_2) + \psi_2^*(\vec{p}_2, \vec{\rho}_2)]\rangle = \exp\left[-\left(\frac{|\vec{p}_1 - \vec{p}_2|}{\rho_o}\right)^{5/3}\right] \tag{15}$$

where ρ_o = transverse coherence length, the diffuse component becomes

$$\Gamma_d(\vec{p}_1, \vec{p}_2) = \frac{R}{\pi L^2} \exp\left[ik \frac{(p_1^2 - p_2^2)}{2L}\right] \int d\vec{\rho}_2 \, \langle |U_i(\vec{\rho}_2)|^2\rangle \times \exp\left[-\frac{ik}{L}(\vec{p}_1 - \vec{p}_2) \cdot \vec{\rho}_2\right] \exp\left[-\left(\frac{|\vec{p}_1 - \vec{p}_2|}{\rho_o}\right)^{5/3}\right] \tag{16}$$

where $p_i = |\vec{p}_i|$.

Using equation (2),

$$\langle |U_i(\rho_1)|^2\rangle = \left(\frac{k}{2\pi L}\right)^2 \iint d\vec{r}_1 d\vec{r}_2 \, \langle U_o(\vec{r}_1) \, U_o^*(\vec{r}_2)\rangle \times \exp\left[\frac{ik|\vec{\rho}_2 - \vec{r}_1|^2}{2L} - \frac{ik|\vec{\rho}_2 - \vec{r}_2|^2}{2L}\right] \times \langle \exp[\psi_1(\vec{\rho}_2, \vec{r}_1) + \psi_1^*(\vec{\rho}_2, \vec{r}_2)]\rangle \tag{17}$$

Substituting equation (1) into equation (17) and using the equivalent of equation (15) gives

$$\langle |U_i(\rho_1)|^2 \rangle = \left(\frac{k}{2\pi L}\right)^2 |U_o|^2 \iint d\vec{r}_1 d\vec{r}_2 \exp\left[-\frac{r_1^2 + r_2^2}{2\alpha_o^2}\right] \times \exp\left[-\frac{ik}{2L}\left(1 - \frac{L}{F}\right)(r_1^2 - r_2^2)\right] \times \exp\left[-\frac{ik}{L}\vec{\rho}_2 \cdot (\vec{r}_1 - \vec{r}_2)\right] \times \exp\left[-\left(\frac{|\vec{r}_1 - \vec{r}_2|}{\rho_o}\right)^{5/3}\right] \qquad (18)$$

where $r_i = |\vec{r}_i|$. Substituting this expression into equation (16) gives a general result for the diffuse component of the mutual coherence function. The resulting expression can be evaluated for the focused case (F = L) giving

$$\Gamma_d(\vec{p}_1, \vec{p}_2) = R|U_o|^2 \frac{\alpha_o^2}{L^2} \exp\left[\frac{ik}{2L}(p_1^2 - p_2^2) - \frac{|\vec{p}_1 - \vec{p}_2|^2}{4\alpha_o^2} - 2\left|\frac{\vec{p}_1 - \vec{p}_2}{\rho_o}\right|^{5/3}\right] \qquad (19)$$

Using once again equations (8) and (12), the specular component is

$$\Gamma_g(\vec{p}_1, \vec{p}_2) = \left(\frac{k}{2\pi L}\right)^2 \sum_{m_1=1}^{M} \sum_{m_2=1}^{M} \iint \vec{d\rho}_1 \vec{d\rho}_2 \langle U_i^*(\vec{\rho}_{m_1}) U_i(\vec{\rho}_{m_2}) \rangle \times \exp\left[-\frac{1}{(\Delta\rho_\omega)^2}\left(|\vec{\rho}_1 - \vec{\rho}_{m_1}|^2 + |\vec{\rho}_2 - \vec{\rho}_{m_2}|^2\right)\right]$$

$$\times \exp\left[\frac{ik}{2L}\left(|\vec{p}_1 - \vec{\rho}_1|^2 - |\vec{p}_2 - \vec{\rho}_2|^2\right)\right]$$

$$\times \langle \exp\left[\psi_2(\vec{p}_1, \vec{\rho}_1) + \psi_2^*(\vec{p}_2, \vec{\rho}_2)\right]\rangle \qquad (20)$$

after having incorporated the assumptions given following equation (12). Noting that

$$\langle \exp\left[\psi_2(\vec{p}_1, \vec{\rho}_1) + \psi_2^*(\vec{p}_2, \vec{\rho}_2)\right]\rangle =$$

$$\exp\left[-D(\vec{p}_1 - \vec{p}_2, \vec{\rho}_1 - \vec{\rho}_2)\right] \qquad (21)$$

where $D(\vec{\rho}_1 - \vec{\rho}_2, \vec{p}_1 - \vec{p}_2)$ is the wave structure function, equation (20) can be rewritten

$$\Gamma_g(\vec{p}_1, \vec{p}_2) = \left(\frac{k}{2\pi L}\right)^2 \exp\left[\frac{ik}{2L}\left(p_1^2 - p_2^2\right)\right]$$

$$\times \sum_{m_1=1}^{M} \sum_{m_2=1}^{M} \langle U_i^*(\vec{\rho}_{m_1})\, U_i(\vec{\rho}_{m_2})\rangle$$

$$\times \iint d\vec{\rho}_1 d\vec{\rho}_2 \exp\left\{-\frac{1}{(\Delta\rho_\omega)^2}\left(|\vec{\rho}_1 - \vec{\rho}_{m_1}|^2 + |\vec{\rho}_2 - \vec{\rho}_{m_2}|^2\right)\right.$$

$$+ \frac{ik}{2L}\left[(\rho_1^2 - 2\vec{p}_1 \cdot \vec{\rho}_1) - (\rho_2^2 - 2\vec{p}_2 \cdot \vec{\rho}_2)\right]$$

$$\left. - D(\vec{p}_1 - \vec{p}_2, \vec{\rho}_1 - \vec{\rho}_2)\right\} \qquad (22)$$

If we make the change of variables

$\vec{\rho} = \vec{\rho}_1 - \vec{\rho}_2$, and

$2\vec{R} = \vec{\rho}_1 + \vec{\rho}_2$,

the integration over $\vec{R}$ can be performed giving

$$\Gamma_g(\vec{p}_1, \vec{p}_2) = \frac{\pi(\Delta\rho_\omega)^2}{2}\left(\frac{k}{2\pi L}\right)^2 \sum_{m_1=1}^{M}\sum_{m_2=1}^{M} \langle U_i^*(\vec{\rho}_{m_1})\, U_i(\vec{\rho}_{m_2})\rangle$$

$$\times \int d\vec{\rho}\ \exp\left\{-\frac{(\Delta\rho_\omega)^2}{8}\left(\frac{k}{L}\right)^2 |\vec{\rho} - \vec{p}|^2\right.$$

$$+ \frac{ik}{2L}\left(\vec{\rho}_{m_1} + \vec{\rho}_{m_2}\right)\cdot(\vec{\rho} - \vec{p})$$

$$- \frac{1}{2(\Delta\rho_\omega)^2}\left|\vec{\rho} - \vec{\rho}_{m_1} + \vec{\rho}_{m_2}\right|^2$$

$$\left. - \frac{ik}{2L}(\vec{p}_1 + \vec{p}_2)\cdot(\vec{\rho} - \vec{p}) - D(\vec{p}, \vec{\rho})\right\} \quad (23)$$

where $\vec{p} = \vec{p}_1 - \vec{p}_2$ and $p = |\vec{p}|$.

In the above developments, it has been implicitly assumed that $(\Delta\rho_\omega)$, the "size" of the glints, is much smaller than the beam at the target. If it can be assumed further that $(\Delta\rho_\omega)$ is small compared with α_o and ρ_o, then in integral expressions such as Eq. (20) all terms are varying extremely slowly with respect to ρ compared to the magnitude of the glint term and the approximation

$$\frac{1}{\pi(\Delta\rho_\omega)^2}\ \exp\left[-\frac{|\vec{\rho} - \vec{\rho}_m|^2}{(\Delta\rho_\omega)^2}\right] \approx \delta(\vec{\rho} - \vec{\rho}_m) \quad (24)$$

is valid. Then equation (20) can be written in the closed form:

$$\Gamma_g(\vec{p}_1, \vec{p}_2) \approx (\Delta\rho_\omega)^4\left(\frac{k}{2L}\right)^2 \sum_{m_1=1}^{M}\sum_{m_2=1}^{M} \langle U_i^*(\vec{\rho}_{m_1})\, U_i(\vec{\rho}_{m_2})\rangle$$

$$\times \exp\left\{\frac{ik}{2L}\left[\left|\vec{\rho}_{m_1} - \vec{p}_1\right|^2 - \left|\vec{\rho}_{m_2} - \vec{p}_2\right|^2\right]\right.$$

$$- \frac{(\Delta\rho_\omega)^2}{8}\left(\frac{k}{L}\right)^2 \left|\vec{\rho}_{m_1} - \vec{\rho}_{m_2} - \vec{p}\right|^2$$

$$\left. - D\left(\vec{p}, \vec{\rho}_{m_1} - \vec{\rho}_{m_2}\right)\right\} \qquad (25)$$

Thus, the mutual coherence function of equation (8) can be evaluated by using equations (19) and (23) or (25) in equation (13).

These expressions can be used to evaluate the mean irradiance at the receiver. For the focused case,

$$\langle I(p)\rangle = \Gamma(\vec{p}, \vec{p})$$

$$= R|U_o|^2 \frac{a_o^2}{L^2} + \frac{(\Delta\rho_\omega)^2}{4}\left(\frac{k}{L}\right)^2 \sum_{m_1=1}^{M}\sum_{m_2=1}^{M} \langle U_i^*(\vec{\rho}_{m_1}) U_i(\vec{\rho}_{m_2})\rangle$$

$$\times \int \rho d\rho\, J_o\left\{\rho\left|\frac{k}{L}\left(\vec{p} - \frac{\vec{\rho}_{m+}}{2}\right) + i\frac{\vec{\rho}_{m-}}{(\Delta\rho_\omega)^2}\right|\right\}$$

$$\times \exp\left\{\frac{(\Delta\rho_\omega)^2}{8}\left(\frac{k}{L}\right)^2 \rho^2 - \frac{\rho^2 + \rho_{m-}^2}{2(\Delta\rho_\omega)^2} - \left(\frac{\rho}{\rho_o}\right)^{5/3}\right\} \qquad (26)$$

where the change of variables

$$\vec{\rho}_{m-} = \vec{\rho}_{m_1} - \vec{\rho}_{m_2}, \text{ and}$$

$$\vec{\rho}_{m+} = \vec{\rho}_{m_1} + \vec{\rho}_{m_2}$$

has been used and the angular integration performed. Using the approximation of equation (24), this can be written in the simplified form

$$\langle I(\vec{p})\rangle = R|U_o|^2 \frac{a_o^2}{L^2}$$

$$+ (\Delta\rho_\omega)^4 \left(\frac{k}{2L}\right)^2 \sum_{m_1=1}^{M} \sum_{m_2=1}^{M} \langle U_i^*(\vec{\rho}_{m_1})\, U_i(\vec{\rho}_{m_2})\rangle$$

$$\times \exp\left\{ \frac{ik}{2L} \vec{\rho}_{m-} \cdot (\vec{\rho}_{m+} - 2\vec{p}) - \frac{(\Delta\rho_\omega)^2}{8} \left(\frac{k}{L}\right)^2 \rho_{m-}^2 - \left(\frac{\rho_{m-}}{\rho_o}\right)^{5/3} \right\} \quad (27)$$

For the special case of a single glint,

$$\langle I(\vec{p})\rangle\Big|_{M=1} = R|U_o|^2 \frac{\alpha_o^2}{L^2} + (\Delta\rho_\omega)^2 \left(\frac{k}{2L}\right)^4 \langle I_i(\vec{\rho}_g)\rangle \quad (28)$$

where $\vec{\rho}_g$ = position of the glint, and

$$\langle I_i(\vec{\rho}_g)\rangle = \langle U_i^*(\vec{\rho}_g)\, U_i(\vec{\rho}_g)\rangle \ .$$

For M = 2 (two glints),

$$\langle I(\vec{p})\rangle\Big|_{M=2} = R|U_o|^2 \frac{\alpha_o^2}{L^2} + (\Delta\rho_\omega)^4 \left(\frac{k}{2L}\right)^4 \Bigg\{ \langle I_i\, \vec{\rho}_{g_1}\rangle + \langle I_i\, \vec{\rho}_{g_2}\rangle$$

$$+ \langle U_i^*(\vec{\rho}_{g_1})\, U_i(\vec{\rho}_{g_2})\rangle$$

$$\times \exp\left[\frac{ik}{2L} (\vec{\rho}_{g_1} - \vec{\rho}_{g_2}) \cdot (\vec{\rho}_{g_1} + \vec{\rho}_{g_2} - 2\vec{p}) \right.$$

$$\left. - \frac{(\Delta\rho_\omega)^2}{8} \left(\frac{k}{L}\right)^2 |\vec{\rho}_{g_1} - \vec{\rho}_{g_2}|^2 - \left(\frac{|\vec{\rho}_{g_1} - \vec{\rho}_{g_2}|}{\rho_o}\right)^{5/3} \right]$$

$$+ \langle U_i^*(\vec{\rho}_{g_2}) U_i(\rho_{g_1})\rangle$$

$$\times \exp\left[\frac{ik}{2L}\left(\vec{\rho}_{g_2} - \vec{\rho}_{g_1}\right) \cdot \left(\vec{\rho}_{g_2} + \vec{\rho}_{g_1} - 2\vec{p}\right)\right.$$

$$\left. - \frac{\left(\Delta\rho_\omega\right)^2}{8}\left(\frac{k}{L}\right)^2\left(|\vec{\rho}_{g_2} - \vec{\rho}_{g_1}|^2\right) - \left(\frac{|\vec{\rho}_{g_2} - \vec{\rho}_{g_1}|}{\rho_o}\right)^{5/3}\right]\Bigg\} \quad (29)$$

C. Covariance of Irradiance

Many of the significant statistical properties of the received field are revealed by an examination of the covariance of irradiance at the receiver.

$$C_I(\vec{p}_1, \vec{p}_2) = \langle I_r(\vec{p}_1)\, I_r(\vec{p}_2)\rangle - \langle I_r(\vec{p}_1)\rangle\langle I_r(\vec{p}_2)\rangle \tag{30}$$

In order to evaluate the covariance of irradiance, it is convenient to focus on each of the two terms on the right hand side of equation (30) separately. The first term is the correlation function of irradiance:

$$B_I(\vec{p}_1, \vec{p}_2) = \langle I_r(\vec{p}_1)\, I_r(\vec{p}_2)\rangle$$

$$= \langle U_r(\vec{p}_1) U_r^*(\vec{p}_1)\, U_r(\vec{p}_2)\, U_r^*(\vec{p}_2)\rangle \,. \tag{31}$$

An expression for this correlation function can be written by applying the extended Huygens-Fresnel principle to the fields scattered from the target. Thus:

$$B_I(\vec{p}_1, \vec{p}_2) = \left(\frac{k}{2\pi L}\right)^4 \iiiint d\vec{\rho}_1 d\vec{\rho}_2 d\vec{\rho}_3 d\vec{\rho}_4 \,\langle U_s(\vec{\rho}_1)\, U_s^*(\vec{\rho}_2)\, U_s(\vec{\rho}_3)\, U_s^*(\vec{\rho}_4)\rangle$$

$$\times \exp\left\{\frac{ik}{2L}\left[|\vec{p}_1 - \vec{\rho}_1|^2 - |\vec{p}_1 - \vec{\rho}_2|^2 + |\vec{p}_2 - \vec{\rho}_3|^2 - |\vec{p}_2 - \vec{\rho}_4|^2\right]\right\}$$

$$\times \langle \exp\left[\psi_2(\vec{p}_1, \vec{\rho}_1) + \psi_2^*(\vec{p}_1, \vec{\rho}_2) + \psi_2(\vec{p}_2, \vec{\rho}_3) + \psi_2^*(\vec{p}_2, \vec{\rho}_4)\right]\rangle \tag{32}$$

Using equations (3) and (11), the fourth order correlation of the scattered field in the integrand of equation (32) can be rewritten as

$$\langle U_s(\vec{\rho}_1)\, U_s^*(\vec{\rho}_2)\, U_s(\vec{\rho}_3)\, U_s^*(\vec{\rho}_4)\rangle = \langle U_d(\vec{\rho}_1)\, U_d^*(\vec{\rho}_2)\, U_d(\vec{\rho}_3)\, U_d^*(\vec{\rho}_4)\rangle$$

$$+ \langle U_d(\vec{\rho}_1)\, U_d^*(\vec{\rho}_2)\, U_g(\vec{\rho}_3)\, U_g^*(\vec{\rho}_4)\rangle$$

$$+ \langle U_g(\vec{\rho}_1)\, U_g^*(\vec{\rho}_2)\, U_d(\vec{\rho}_3)\, U_d^*(\vec{\rho}_4)\rangle$$

$$+ \langle U_g(\vec{\rho}_1)\, U_d^*(\vec{\rho}_2)\, U_d(\vec{\rho}_3)\, U_g^*(\vec{\rho}_4)\rangle$$

$$+ \langle U_d(\vec{\rho}_1)\, U_g^*(\vec{\rho}_2)\, U_g(\vec{\rho}_3)\, U_d^*(\vec{\rho}_4)\rangle$$

$$+ \langle U_g(\vec{\rho}_1)\, U_g^*(\vec{\rho}_2)\, U_g(\vec{\rho}_3)\, U_g^*(\vec{\rho}_4)\rangle$$

$$\equiv \sum_{n=1}^{6} A_n(\vec{\rho}_1, \vec{\rho}_2, \vec{\rho}_3, \vec{\rho}_4) \tag{33}$$

where the A_n are defined by equation (33). Then the correlation of irradiance at the receiver can be written as the sum of six terms:

$$B_I(\vec{p}_1, \vec{p}_2) = \sum_{n=1}^{6} B_{I_n}(\vec{p}_1, \vec{p}_2) \tag{34}$$

where from equations (32) and (33),

$$B_{I_n}(\vec{p}_1, \vec{p}_2) = \left(\frac{k}{2\pi L}\right)^4 \iiiint d\vec{\rho}_1 d\vec{\rho}_2 d\vec{\rho}_3 d\vec{\rho}_4\, A_n(\vec{\rho}_1, \vec{\rho}_2, \vec{\rho}_3, \vec{\rho}_4)$$

$$\times \exp\left\{\frac{ik}{2L}\left[|\vec{p}_1 - \vec{\rho}_1|^2 - |\vec{p}_1 - \vec{\rho}_2|^2 + |\vec{p}_2 - \vec{\rho}_3|^2 - |\vec{p}_2 - \vec{\rho}_4|^2\right]\right\}$$

$$\times \langle \exp\left[\psi_2(\vec{p}_1, \vec{\rho}_1) + \psi_2^*(\vec{p}_1, \vec{\rho}_2) + \psi_2(\vec{p}_2, \vec{\rho}_3) + \psi_2^*(\vec{p}_2, \vec{\rho}_4)\right]\rangle \tag{35}$$

The fourth order mutual coherence function due to turbulence in equation (32) is defined as

$$H(\vec{p}_1, \vec{p}_2; \vec{\rho}_1, \vec{\rho}_2, \vec{\rho}_3, \vec{\rho}_4) = \langle \exp\left[\psi_2(\vec{p}_1, \vec{\rho}_1) + \psi_2^*(\vec{p}_1, \vec{\rho}_2) + \psi_2(\vec{p}_2, \vec{\rho}_3) + \psi_2(\vec{p}_2, \vec{\rho}_4)\right]\rangle$$

$$= \exp\left\{-\frac{1}{2}\left[D_\psi(\vec{\rho}_1 - \vec{\rho}_2) - D_\psi(\vec{p}_1 - \vec{p}_2, \vec{\rho}_1 - \vec{\rho}_3)\right.\right.$$

$$+ D_\psi(\vec{\rho}_1 - \vec{\rho}_2, \vec{\rho}_1 - \vec{\rho}_4) + D_\psi(\vec{\rho}_1 - \vec{\rho}_2, \vec{\rho}_2 - \vec{\rho}_3)$$

$$- D_\psi(\vec{\rho}_1 - \vec{\rho}_2, \vec{\rho}_2 - \vec{\rho}_4) + D_\psi(\vec{\rho}_3 - \vec{\rho}_4)\Big]$$

$$+ 2C_\ell(\vec{\rho}_1 - \vec{\rho}_2, \vec{\rho}_1 - \vec{\rho}_3) + 2C_\ell(\vec{\rho}_1 - \vec{\rho}_2, \vec{\rho}_2 - \vec{\rho}_4)\Big\} \tag{36}$$

where D_ψ and C_ℓ are the wave structure function and the log amplitude covariance function for a spherical wave, respectively.

Using the notation of equation (35) along with equations (10) and (11), the six terms making up the correlation function of irradiance at the receiver may be written. Using

$$\begin{aligned} A_1(\vec{\rho}_1, \vec{\rho}_2, \vec{\rho}_3, \vec{\rho}_4) &= \langle U_d(\vec{\rho}_1)\, U_d^*(\vec{\rho}_2)\, U_d(\vec{\rho}_3)\, U_d^*(\vec{\rho}_4)\rangle \\ &= \langle U_d(\vec{\rho}_1)\, U_d^*(\vec{\rho}_2)\rangle\langle U_d(\vec{\rho}_3)\, U_d^*(\vec{\rho}_4)\rangle \\ &\quad + \langle U_d(\vec{\rho}_1)\, U_d^*(\vec{\rho}_4)\rangle\langle U_d^*(\vec{\rho}_2)\, U_d(\vec{\rho}_3)\rangle \\ &= \left(\frac{4\pi}{k^2}\right)^2 \Big\{ \langle I_d(\vec{\rho}_1)\rangle\langle I_d(\vec{\rho}_3)\rangle\, \delta(\vec{\rho}_1 - \vec{\rho}_2)\, \delta(\vec{\rho}_3 - \vec{\rho}_4) \\ &\quad + \langle I_d(\vec{\rho}_1)\rangle\langle I_d(\vec{\rho}_3)\rangle\, \delta(\vec{\rho}_1 - \vec{\rho}_4)\, \delta(\vec{\rho}_3 - \vec{\rho}_2)\Big\} \end{aligned}$$

in equation (35) gives

$$\begin{aligned} B_{I_1}(\vec{\rho}_1, \vec{\rho}_2) = \frac{1}{\pi^2 L^4} \iint d\vec{\rho}_2 d\vec{\rho}_4\, \langle I_d(\vec{\rho}_2)\rangle\langle I_d(\rho_4)\rangle \\ \Big\{ \exp\left[4C_\ell(\vec{\rho}_1 - \vec{\rho}_2, \vec{\rho}_2 - \vec{\rho}_4)\right] + \exp\left[\frac{ik}{L}(\vec{\rho}_1 - \vec{\rho}_2)\cdot(\vec{\rho}_2 - \vec{\rho}_4)\right] \\ H(\vec{\rho}_1, \vec{\rho}_2; \vec{\rho}_4, \vec{\rho}_2, \vec{\rho}_2, \vec{\rho}_4)\Big\} \end{aligned} \tag{37}$$

Using $A_2(\vec{\rho}_1, \vec{\rho}_2, \vec{\rho}_3, \vec{\rho}_4) = \langle U_d(\vec{\rho}_1)\, U_d^*(\vec{\rho}_2)\, U_g(\vec{\rho}_3)\, U_g^*(\vec{\rho}_4)\rangle$

$$= \langle U_d(\vec{\rho}_1)\, U_d^*(\vec{\rho}_2)\rangle \langle U_g(\vec{\rho}_3)\, U_g^*(\vec{\rho}_4)\rangle$$

$$= \frac{4\pi}{k^2} \langle I_d(\vec{\rho}_1)\rangle \langle U_g(\vec{\rho}_3)\, U_g^*(\vec{\rho}_4)\rangle\, \delta(\vec{\rho}_1 - \vec{\rho}_2)$$

in equation (35) gives

$$B_{I_2}(\vec{p}_1, \vec{p}_2) = \frac{k^2}{4\pi^3 L^4} \iiint d\vec{\rho}_2 d\vec{\rho}_3 d\vec{\rho}_4 \langle I_d(\vec{\rho}_2)\rangle \langle U_g(\vec{\rho}_3)\, U_g^*(\vec{\rho}_4)\rangle$$

$$\times \exp\left[\frac{ik}{2L}(\vec{\rho}_3 + \vec{\rho}_4 - 2\vec{p}_2) \cdot (\vec{\rho}_3 - \vec{\rho}_4)\right]$$

$$\times H(\vec{p}_1, \vec{p}_2; \rho_2, \rho_2, \rho_3, \rho_4) \qquad (38)$$

Using $A_3(\vec{\rho}_1, \vec{\rho}_2, \vec{\rho}_3, \vec{\rho}_4) = \langle U_g(\vec{\rho}_1)\, U_g^*(\vec{\rho}_2)\, U_d(\vec{\rho}_3)\, U_d^*(\vec{\rho}_4)\rangle$

$$= \langle U_g(\vec{\rho}_1)\, U_g^*(\vec{\rho}_2)\rangle \langle U_d(\vec{\rho}_3)\, U_d^*(\vec{\rho}_4)\rangle$$

$$= \frac{4\pi}{k^2} \langle U_g(\vec{\rho}_1)\, U_g^*(\vec{\rho}_2)\rangle \langle I_d(\vec{\rho}_3)\rangle\, \delta(\vec{\rho}_3 - \vec{\rho}_4)$$

in equation (35) gives

$$B_{I_3}(\vec{p}_1, \vec{p}_2) = \frac{k^2}{4\pi^3 L^4} \iiint d\vec{\rho}_1 d\vec{\rho}_2 d\vec{\rho}_4 \langle I_d(\vec{\rho}_4)\rangle \langle U_g(\vec{\rho}_1)\, U_g^*(\vec{\rho}_2)\rangle$$

$$\times \exp\left[\frac{ik}{2L}(\vec{\rho}_1 + \vec{\rho}_2 - 2\vec{p}_1) \cdot (\vec{\rho}_1 - \vec{\rho}_2)\right]$$

$$\times H(\vec{p}_1, \vec{p}_2; \vec{\rho}_1, \vec{\rho}_2, \vec{\rho}_4, \vec{\rho}_4) \qquad (39)$$

Using $A_4(\vec{\rho}_1, \vec{\rho}_2, \vec{\rho}_3, \vec{\rho}_4) = \langle U_g(\vec{\rho}_1)\, U_d^*(\vec{\rho}_2)\, U_d(\vec{\rho}_3)\, U_g^*(\vec{\rho}_4)\rangle$

$$= \langle U_g(\vec{\rho}_1)\, U_g^*(\vec{\rho}_4)\rangle \langle U_d^*(\vec{\rho}_2)\, U_d(\vec{\rho}_3)\rangle$$

$$= \frac{4\pi}{k^2} \langle U_g(\vec{\rho}_1)\, U_g^*(\vec{\rho}_4)\rangle \langle I_d(\vec{\rho}_3)\rangle\, \delta(\vec{\rho}_3 - \vec{\rho}_2)$$

in equation (35) gives

$$B_{I_4}(\vec{p}_1, \vec{p}_2) = \frac{k^2}{4\pi^3 L^4} \iiint d\vec{\rho}_1 d\vec{\rho}_2 d\vec{\rho}_4 \; \langle I_d(\vec{\rho}_4)\rangle \langle U_g(\vec{\rho}_1)\rangle \langle U_g^*(\vec{\rho}_2)\rangle$$

$$\times \exp\left\{\frac{ik}{2L}\left[(\vec{\rho}_1 + \vec{\rho}_2 - 2\vec{p}_1)\cdot(\vec{\rho}_1 - \vec{\rho}_2) + (\vec{\rho}_2 + \vec{\rho}_4 - 2\vec{p}_2)\right.\right.$$

$$\left.\left.\cdot(\vec{\rho}_2 - \vec{\rho}_4)\right]\right\} \times H(\vec{p}_1, \vec{p}_2; \vec{\rho}_1, \vec{\rho}_2, \vec{\rho}_2, \vec{\rho}_4,) \qquad (40)$$

Using $A_5(\vec{\rho}_1, \vec{\rho}_2, \vec{\rho}_3, \vec{\rho}_4) = \langle U_d(\vec{\rho}_1)\, U_g^*(\vec{\rho}_2)\, U_g(\vec{\rho}_3)\, U_d^*(\vec{\rho}_4)\rangle$

$$= U_d(\vec{\rho}_1)\, U_d^*(\vec{\rho}_4)\rangle\langle U_g^*(\vec{\rho}_2)\, U_g(\vec{\rho}_3)\rangle$$

$$= \frac{4\pi}{k^2} \langle I_d(\vec{\rho}_1)\rangle \langle U_g^*(\vec{\rho}_2)\, U_g(\vec{\rho}_3)\rangle\, \delta(\vec{\rho}_1 - \vec{\rho}_4)$$

in equation (35) gives

$$B_{I_5}(\vec{p}_1, \vec{p}_2) = \frac{k^2}{4\pi^3 L^4} \iiint d\vec{\rho}_2 d\vec{\rho}_3 d\vec{\rho}_4 \; \langle I_d(\vec{\rho}_2)\rangle \langle U_g^*(\vec{\rho}_2)\, U_g(\vec{\rho}_3)\rangle$$

$$\times \exp\left\{\frac{ik}{2L}\left[(\vec{\rho}_4 + \vec{\rho}_2 - 2\vec{p}_1)\cdot(\vec{\rho}_4 - \vec{\rho}_2) + (\vec{\rho}_3 + \vec{\rho}_4 - 2\vec{p}_2)\right.\right.$$

$$\left.\left.\cdot(\vec{\rho}_3 - \vec{\rho}_4)\right]\right\} \times H(\vec{p}_1, \vec{p}_2; \vec{\rho}_4, \vec{\rho}_2, \vec{\rho}_3, \vec{\rho}_4) \qquad (41)$$

Using $A_6(\vec{\rho}_1, \vec{\rho}_2, \vec{\rho}_3, \vec{\rho}_4) = \langle U_g(\vec{\rho}_1)\, U_g^*(\vec{\rho}_2)\, U_g(\vec{\rho}_3)\, U_g^*(\vec{\rho}_4)\rangle$

in equation (35) gives

$$B_{I_6}(\vec{p}_1, \vec{p}_2) = \left(\frac{k}{2\pi L}\right)^4 \iiiint d\vec{\rho}_1 d\vec{\rho}_2 d\vec{\rho}_3 d\vec{\rho}_4 \; \langle U_g(\vec{\rho}_1)\, U_g^*(\vec{\rho}_2)\, U_g(\vec{\rho}_3)\; U_g^*(\vec{\rho}_4)\rangle$$

$$\times \exp\left\{\frac{ik}{2L}\left[|\vec{p}_1 - \vec{\rho}_1|^2 - |\vec{p}_1 - \vec{\rho}_2|^2 + |\vec{p}_2 - \vec{\rho}_3|^2 - |\vec{p}_2 - \vec{\rho}_4|^2\right]\right\}$$

$$\times H(\vec{p}_1, \vec{p}_2; \vec{\rho}_1, \vec{\rho}_2, \vec{\rho}_3, \vec{\rho}_4) \qquad (42)$$

The second term on the right hand side of equation (30) can be expanded using

$$\langle I_r(\vec{p})\rangle = \langle I_d(\vec{p}) + I_g(\vec{p})\rangle$$

$$= \langle I_d(\vec{p})\rangle + \langle I_g(\vec{p})\rangle \tag{43}$$

where $\langle I_d(\vec{p})\rangle$ and $\langle I_g(\vec{p})\rangle$ may be obtained by setting $\vec{p}_1 = \vec{p}_2 = \vec{p}$ in equations (19) and (22) respectively. Using equation (43) then,

$$\langle I_r(\vec{p}_1)\rangle\langle I_r(\vec{p}_2)\rangle = \langle I_d(\vec{p}_1)\rangle\langle I_d(\vec{p}_2)\rangle + \langle I_d(\vec{p}_1)\rangle\langle I_g(\vec{p}_2)\rangle$$

$$+ \langle I_g(\vec{p}_1)\rangle\langle I_g(\vec{p}_2)\rangle + \langle I_g(\vec{p}_1)\rangle\langle I_g(\vec{p}_2)\rangle \tag{44}$$

An expression for the covariance of irradiance can be written using the following definitions:

$$C_I(\vec{p}_1, \vec{p}_2)_d = \langle I_d(\vec{p}_1)\, I_d(\vec{p}_2)\rangle - \langle I_d(\vec{p}_1)\rangle\langle I_d(\vec{p}_2)\rangle$$

$$= B_{I_1}(\vec{p}_1, \vec{p}_2) - \langle I_d(\vec{p}_1)\rangle\langle I_d(\vec{p}_2)\rangle, \tag{45}$$

$$C_I(\vec{p}_1, \vec{p}_2)_g = \langle I_g(\vec{p}_1)\, I_g(\vec{p}_2)\rangle - \langle I_g(\vec{p}_1)\rangle\langle I_g(p_2)\rangle$$

$$= B_{I_6}(\vec{p}_1, \vec{p}_2) - \langle I_g(\vec{p}_1)\rangle\langle I_g(\vec{p}_2)\rangle, \tag{46}$$

$$C_{I_dI_g}(\vec{p}_1, \vec{p}_2) = \langle I_d(\vec{p}_1)\, I_g(\vec{p}_2)\rangle - \langle I_d(\vec{p}_1)\rangle\langle I_g(\vec{p}_2)\rangle$$

$$= B_{I_2}(\vec{p}_1, \vec{p}_2) - \langle I_d(\vec{p}_1)\rangle\langle I_g(\vec{p}_2)\rangle, \tag{47}$$

$$C_{I_dI_g}(\vec{p}_2, \vec{p}_1) = \langle I_d(\vec{p}_2)\, I_g(\vec{p}_1)\rangle - \langle I_d(\vec{p}_2)\rangle\langle I_g(\vec{p}_1)\rangle$$

$$= B_{I_3}(\vec{p}_1, \vec{p}_2) - \langle I_d(\vec{p}_2)\rangle\langle I_g(\vec{p}_1)\rangle, \tag{48}$$

$$C_{U_{dg}}(\vec{p}_1, \vec{p}_2) = \langle U_d(\vec{p}_1)\, U_g^*(\vec{p}_1)\, U_d^*(\vec{p}_2)\, U_g(\vec{p}_2)\rangle$$

$$= B_{I_4}(\vec{p}_1, \vec{p}_2), \tag{49}$$

and

$$\langle U_g(\vec{\rho}_1)\, U_g^*(\vec{\rho}_2)\, U_g(\vec{\rho}_3)\, U_g^*(\vec{\rho}_4)\rangle$$

$$= \sum_{m_1=1}^{M} \sum_{m_2=1}^{M} \sum_{m_3=1}^{M} \sum_{m_4=1}^{M} \langle U_i^*(\vec{\rho}_{m_1})\, U_i(\vec{\rho}_{m_2})\, U_i^*(\vec{\rho}_{m_3})\, U_i(\vec{\rho}_{m_4})\rangle$$

$$\times \exp\left\{-\frac{1}{(\Delta\rho_w)^2}\left[(\vec{\rho}_1 - \vec{\rho}_{m_1})^2 + (\vec{\rho}_2 - \vec{\rho}_{m_2})^2 + (\vec{\rho}_3 - \vec{\rho}_{m_3})^2 + (\vec{\rho}_4 - \vec{\rho}_{m_4})^2\right]\right\} \tag{50}$$

where

$$\langle U_i^*(\vec{\rho}_{m_1})\, U_i(\vec{\rho}_{m_2})\, U_i^*(\vec{\rho}_{m_3})\, U_i(\vec{\rho}_{m_4})\rangle$$

$$= \left(\frac{k}{2\pi L}\right) \iiiint d\vec{r}_1 d\vec{r}_2 d\vec{r}_3 d\vec{r}_4\, U^*(\vec{r}_1)\, U(\vec{r}_2)\, U^*(\vec{r}_3)\, U(\vec{r}_4)$$

$$\times \exp\left\{-\frac{ik}{2L}\left[(\vec{\rho}_{m_1} - \vec{r}_1)^2 - (\vec{\rho}_{m_2} - \vec{r}_2)^2 + (\vec{\rho}_{m_3} - \vec{r}_3)^2 - (\vec{\rho}_{m_4} - \vec{r}_4)^2\right]\right\}$$

$$\times H\left(\vec{\rho}_{m_1}, \vec{\rho}_{m_2}, \vec{\rho}_{m_3}, \vec{\rho}_{m_4}; \vec{r}_1, \vec{r}_2, \vec{r}_3, \vec{r}_4\right) . \tag{51}$$

The covariance of irradiance becomes

$$C_I(\vec{p}_1, \vec{p}_2) = C_I(\vec{p}_1, \vec{p}_2)_d + C_I(\vec{p}_1, \vec{p}_2)_g + C_{I_d I_g}(\vec{p}_1, \vec{p}_2)$$

$$+ C_{I_d I_g}(\vec{p}_2, \vec{p}_1) + C_{u_{dg}}(\vec{p}_1, \vec{p}_2) + C^*_{u_{dg}}(\vec{p}_1, \vec{p}_2) . \tag{52}$$

The variance of irradiance can be obtained from equation (52) by setting $\vec{p}_1 = \vec{p}_2 = \vec{p}$ and is

$$\sigma_I^2(\vec{p}) = \sigma_{I_d}{}^2(\vec{p}) + \sigma_{I_g}{}^2(p) + 2C_{I_dI_g}(\vec{p}, \vec{p}) + 2C_{u_{dg}}(\vec{p}, \vec{p}) \qquad (53)$$

D. Speckle Patterns With Reduced Source Coherence

In this section, the effect of reduced temporal coherence[8,9] of the source is considered. Following the development of the previous sections, and using the definitions given there, the two frequency mutual intensity function is

$$\Gamma_f(\vec{p}_1, k_1; \vec{p}_2, k_2) = \langle U_r(\vec{p}_1, k_1)\, U_r^*(\vec{p}_2, k_2)\rangle$$

$$= \frac{k_1 k_2}{(2\pi L)^2} \iint d\vec{\rho}_1 d\vec{\rho}_2 \left\langle \left\{ -R^{1/2} U_i(\vec{\rho}_1, k_1) + \sum_{m_1=1}^{M} U_i^*\left(\vec{\rho}_{m_1}, k_1\right) \exp\left[-\frac{\left(\vec{\rho} - \vec{\rho}_{m_1}\right)^2}{\left(\Delta\rho_w\right)^2} \right] \right\} \right.$$

$$\times \left\{ -R^{1/2}\, U_i^*(\vec{\rho}_2, k_2) + \sum_{m_2=1}^{M} U_i\left(\vec{\rho}_{m_2}, k_2\right) \exp\left[-\frac{\left(\vec{\rho} - \vec{\rho}_{m_2}\right)^2}{\left(\Delta\rho_w\right)^2} \right] \right\} \Bigg\rangle$$

$$\times \exp\left[\frac{ik_1}{2L} (\vec{p}_1 - \vec{\rho}_1)^2 - \frac{ik_2}{2L} (\vec{p}_2 - \vec{\rho}_2)^2 \right]$$

$$\times \langle \exp\left[\psi(\vec{p}_1, \vec{\rho}_1, k_1) + \psi^*(\vec{p}_2, \vec{\rho}_2, k_2) \right] \rangle \qquad (54)$$

where $k_i = \frac{2\pi}{\lambda_i}$,

λ_i = wavelength.

In order to simplify the expression in equation (54), the ensemble averages implicit in the integral can be evaluated. For the diffusely scattered radiation,

$$\langle U_d(\vec{\rho}_1, k_1)\, U_d^*(\vec{\rho}_2, k_2)\rangle = \frac{4\pi R}{k_1^2}\,\beta\,\langle I_i(\vec{\rho}_1, k_1)\rangle\,\delta(\vec{\rho}_1 - \vec{\rho}_2)\,\delta(k_1 - k_2) \quad (55)$$

where β is a normalization constant that will be evaluated below. It has been suggested that the log amplitude covariance function and the wave structure vary weakly with wave number.[10] We extend this to the narrow band spherical wave for the purposes of this calculation and assume that

$$\langle \exp\left[\psi(\vec{p}_1, \vec{\rho}_1, k_1) + \psi^*(\vec{p}_2, \rho_2, k_2)\right]\rangle$$

can be approximated by

$$\langle \exp\left[\psi(\vec{p}_1, \vec{\rho}_1, k_o) + \psi^*(\vec{p}_2, \vec{\rho}_2, k_o)\right]\rangle = \exp\left[-\frac{1}{2} D(\vec{p}_2 - \vec{p}_1, \vec{\rho}_2 - \vec{\rho}_1, k_o\right] \quad (56)$$

where k_o is the mean wave number. For the coherently scattered radiation (from the glints), we have for the focused case

$$\langle U_g^*\left(\vec{\rho}_{m_1}, k_1\right)\, U_g\left(\vec{\rho}_{m_2}, k_2\right)\rangle = \frac{k_1 k_2}{\pi}\,\frac{\alpha_o^2\, U_o^2}{(2L)^2}\,\exp\left\{-\left(\frac{\alpha_o}{2L}\right)^2 \left(k_1\vec{\rho}_{m_1} - k_2\vec{\rho}_{m_2}\right) + \frac{ik_1}{2L}\,\rho_{m_1}^2 - \frac{ik_2}{2L}\,\rho_{m_2}^2\right\}$$

$$\times \int d\vec{r}\,\exp\left[-\frac{r^2}{4\alpha_o^2} - i\,\frac{\vec{r}}{L}\left(k_1\vec{\rho}_{m_1} + k_2\vec{\rho}_{m_2}\right) - \frac{1}{2} D\left(\vec{\rho}_{m_2} - \vec{\rho}_{m_1}, \vec{r}, k_o\right)\right] \quad (57)$$

Using equations (55), (56), and (57) along with equation (11), we can write the two frequency mutual intensity as

$$\Gamma_f(\vec{p}_1, k_1; \vec{p}_2, k_2) = \Gamma_{df}(\vec{p}_1, k_1; \vec{p}_2, k_2) + \Gamma_{gf}(\vec{p}_1, k_1; \vec{p}_2, k_2) \qquad (58)$$

where

$$\Gamma_{df}(\vec{p}_1, k_1; \vec{p}_2, k_2) = \beta R \frac{k_2}{k_1} \frac{\alpha_o^2 U_o^2}{L^2} \exp\left\{\frac{ik_1}{2L} p_1^2 - \frac{ik_2}{2L} p_2^2 - \frac{\rho_o}{4\alpha_o^2} - \frac{p_o}{\rho_o}^{5/3} - \left|\frac{\vec{p}_2 - \vec{p}_1}{\rho_o}\right|^{5/3}\right\} \times \delta(k_1 - k_2) \qquad (59)$$

is the diffuse contribution to the mutual intensity,

$$p_o = \frac{1}{k_1} \left|k_1\vec{p}_1 - k_2\vec{p}_2\right|,$$

and the assumption has been made that

$$\exp\left[\frac{i\rho_1^2}{2L} (k_1 - k_2)\right] \approx 1;$$

and where

$$\Gamma_{gf}(\vec{p}_1, k_1; \vec{p}_2, k_2) = \frac{\Delta\rho_w^4 k_1 k_2}{(2L)^2} \exp\left[\frac{i}{2L} (k_1\rho_1^2 - k_2\rho_2^2)\right]$$

$$\times \sum_{m_1=1}^{M} \sum_{m_2=1}^{M} \left\langle U_g\left(\vec{\rho}_{m_1}, k_1\right) U_g^*\left(\vec{\rho}_{m_1}, k_1\right)\right\rangle$$

$$\times \exp\left[\frac{ik_1}{2L} \left(\rho_{m_1}^2 - 2\vec{p}_1\cdot\vec{\rho}_{m_1}\right) - \frac{ik_2}{2L} \left(\rho_{m_2}^2 - 2\vec{p}_2\cdot\vec{\rho}_{m_2}\right)\right.$$

$$\left. - \frac{1}{2} D\left(\vec{p}_2 - \vec{p}_1, \vec{\rho}_{m_2} - \vec{\rho}_{m_1}, k_o\right)\right] \qquad (60)$$

is the contribution from the specular portion of the target.

The mutual intensity at the receiver is the integral of equation (58) over the appropriate spectral distribution of the source. Thus

$$\Gamma_f(\vec{p}_1, \vec{p}_2) = \iint dk_1 dk_2 \left[\Gamma_{df}(\vec{p}_1, k_1; \vec{p}_2, k_2) + \Gamma_{gf}(\vec{p}_1, k_1; \vec{p}_2, k_2)\right] \times S(k_1)\, S(k_2)$$

$$= \Gamma_{df}(\vec{p}_1, \vec{p}_2) + \Gamma_{gf}(\vec{p}_1, \vec{p}_2) \tag{61}$$

If the source has a gaussian spectral density with r.m.s. deviation W and mean wave number k_o, then

$$S(k) = \frac{1}{\sqrt{2\pi}W} \exp\left[-\frac{(k - k_o)^2}{2W^2}\right] \tag{62}$$

Using this assumption, the diffuse contribution to the mutual intensity at the receiver is

$$\Gamma_{df}(\vec{p}_1, \vec{p}_2) = \frac{\beta R}{2\sqrt{\pi}W} \frac{\alpha_o^2\, U_o^2}{L^2} \exp\left[-\frac{W^2(p_1^2 - p_2^2)}{16\, L^2} - \frac{|\vec{p}_2 - \vec{p}_1|^2}{4\alpha_o^2} - 2\left|\frac{\vec{p}_2 - \vec{p}_1}{\rho_o}\right|^{5/3} + \frac{ik_o}{2L}(p_1^2 - p_2^2)\right] \tag{63}$$

Comparing this with previous results in the limit of $W \to 0$, the normalization constant can be evaluated.

$$\beta = 2\sqrt{\pi}W \tag{64}$$

In order to simplify the evaluation of the glint contribution to the mutual intensity, the parameters associated with the Argon ion laser source, namely $k_o = 1.29 \times 10^7$, $\Delta k = 209$ and consequently $\frac{\Delta k}{k} \tilde{=} 1.63 \times 10^{-5}$, are considered. Making the change of variables, $k_1 = k_1$ and $k_2 = k_1 + \Delta k$, the following approximations are useful:

$$\left(\frac{a_o}{2L}\right)^2 \left[k_1\vec{\rho}_{m_1} - (k_1 + \Delta k)\,\vec{\rho}_{m_2}\right]^2 \cong \left(\frac{\alpha_o}{2L}\right)^2 k_1^2 \left(\vec{\rho}_{m_1} - \vec{\rho}_{m_2}\right)^2 ,$$

$$\frac{i\vec{r}}{L} \cdot \left[k_1\vec{\rho}_{m_1} + (k_1 + \Delta k)\,\vec{\rho}_{m_2}\right] \cong \frac{i\vec{r}}{L} \cdot \left[k_1\left(\vec{\rho}_{m_1} + \vec{\rho}_{m_2}\right)\right] \quad , \text{ and}$$

$$\frac{ik_1}{2L}\,\rho_{m_1}^2 - \frac{i(k_1 + \Delta k)}{2L}\,\rho_{m_2}^2 \cong \frac{ik_1}{2L}\left(\rho_{m_1}^2 - \rho_{m_2}^2\right) .$$

This assumes that ρ_{m_1} and ρ_{m_2} are on the order of a centimeter and ignores terms on the order of 10^{-5}. Using these approximations and after considerable manipulation,

$$\Gamma_{gf}(\vec{p}_1, \vec{p}_2) = \left[\frac{(\Delta\rho_w)k_o}{2L}\right]^4 \frac{\alpha_o^2\, U_o^2}{\pi}$$

$$\times \sum_{m_1=1}^{M} \sum_{m_2=1}^{M} \int d\vec{r}\, \frac{\exp\left[-\frac{1}{2} D\left(\vec{p}_2 - \vec{p}_1,\ \vec{\rho}_{m_2} - \vec{\rho}_{m_1}\right)\right]}{\sqrt{1 + 2\left(\frac{\alpha_o}{2L}\right)^2 \rho_{m_{21}}^2\, W^2}}$$

$$\times \exp\left[-\frac{r^2}{4\alpha_o^2} - \frac{1}{2} D\left(\vec{\rho}_{m_2} - \vec{\rho}_{m_1},\ -\vec{r}\right) + \frac{-\left(\frac{\alpha_o}{2L}\right)^2 \rho_{m_{21}}^2\, k_o^2 - \frac{\rho_r^4 W^2}{8L^2} + i\frac{k_o \rho_r^2}{2L}}{1 + 2\left(\frac{\alpha_o}{2L}\right)^2 \rho_{m_{21}}^2\, W^2}\right] \qquad (65)$$

where

$$\rho_{m_{21}}^2 = \left|\vec{\rho}_{m_2} - \vec{\rho}_{m_1}\right|^2, \text{ and}$$

$$\rho_r^2 = \left[\left(\vec{\rho}_{m_1} - \vec{p}_1\right)^2 - \left(\vec{\rho}_{m_2} - \vec{p}_2\right)^2 + \left(\vec{\rho}_{m_1} + \vec{\rho}_{m_2}\right) \cdot \left(\vec{\rho}_{m_1} - \vec{\rho}_{m_2} - 2\vec{r}\right)\right]$$

Following this same approach, expressions for the mean and related second moments can be evaluated, where

$$\langle I(\vec{p})\rangle = \int S(k)\ \langle I(\vec{p},k)\rangle\ dk \tag{66}$$

$$\langle I^2(\vec{p})\rangle = \iint S(k_1)\ S(k_2)\ \langle I(\vec{p},k_1)I(\vec{p},k_2)\rangle\ dk_1 dk_2 \tag{67}$$

$$\langle I(\vec{p}_1,\vec{p}_2)\rangle = \iint S(k_1)\ S(k_2)\ \langle I(\vec{p}_1,k_1)I(\vec{p}_2,k_2)\rangle\ dk_1 dk_2 \tag{68}$$

As in the case of the coherent, or monochromatic, source, these expressions must be evaluated numerically.

III. Numerical Evaluation

In addition to the numerical techniques described previously,[11] the following additional methods were used to evaluate the expressions developed in Section II:

- The scotchlite was assumed to be equivalent to a diffuse surface with a gain of 1000.
- In the evaluation of $\sigma_{I_g}^2$ in Eq. 53, we used experimental data for the variance of a focused gaussian beam.[12]

The principal results are associated with the normalized variance of irradiance for a coherent source and a target consisting of a diffuse surface with a single glint. In particular, it has been determined that the normalized variance of irradiance can be on the order of 3. This corresponds to fluctuations in the received irradiance that are greatly enhanced over those present for a diffuse target alone. These enhanced fluctuations may have a significant impact on systems operating in this geometry.

Table I is a typical example of the results of these calculations, showing a peak in the normalized variance of irradiance of 3.3. The parameters used in this calculation are:

$L = 500$ m (path length),

$\lambda = 488$ nm (wavelength),

$\alpha_o = 1.35$ cm (radius of transmitter beam),

$\alpha_g = 0.19$ mm (radius of glint),

and both the glint and the received irradiance are located on the optical axis.

TABLE I

NORMALIZED VARIANCE OF IRRADIANCE ($\sigma_{I_N}^2$)

DIFFUSE TARGET WITH SINGLE GLINT

C_N^2	$\sigma_{I_N}^2$	$\frac{\langle I_g \rangle}{\langle I_d \rangle}$
5×10^{-16}	.090075	25.895
10^{-15}	.14643	24.685
2×10^{-15}	.35566	22.542
5×10^{-15}	1.0767	17.742
10^{-14}	1.9127	12.909
1.5×10^{-14}	2.6526	10.059
2×10^{-14}	3.3154	8.434
3×10^{-14}	3.1741	6.0089
5×10^{-14}	2.7002	3.9666
10^{-13}	2.1533	2.1015
2×10^{-13}	1.6054	.72014
5×10^{-13}	1.1498	.029616
10^{-12}	1.0921	.000145

C_N^2 = Index of refraction structure constant

$\langle I_g \rangle$ = Mean irradiance from glint; $\langle I_d \rangle$ = Mean irradiance from diffuse portion of target

Note that at low turbulence levels (small C_N^2), the glint dominates the received irradiance, i.e. $\frac{\langle I_g \rangle}{\langle I_d \rangle} >> 1$, while at high turbulence levels, the diffusely scattered light dominates the received irradiance, $\frac{\langle I_g \rangle}{\langle I_d \rangle} << 1$. Thus we expect to see the normalized variance of irradiance return to unity at high integrated path turbulence as for a diffuse target alone.

Figures 2 through 6 illustrate the results of the numerical evaluation. Figure 2 shows the results of previous work for a coherent source and a diffuse target for purposes of reference. The solid curve is a numerical result, and experimental measurements are superimposed on the graph. Several features of this curve are of interest. At low turbulence levels, $\sigma_{I_N}^2 = 1$ due to the diffuse nature of the target. At high turbulence levels, $\sigma_{I_N}^2 = 1$ also. This is the familiar saturation region, and for this particular target the normalized variance returns to unity. At intermediate levels of turbulence, $\sigma_{I_N}^2$ peaks up at approximately 1.25. This peak is due to the log amplitude terms in the mutual coherence function as described previously.

Figure 3 illustrates the effect on $\sigma_{I_N}^2$ with the addition of a glint or specular component to the target. For this case, the glint is located 1 cm off axis; that is, the glint is displaced by 1 cm from the center of the focused gaussian beam on the target. (For no turbulence the $\frac{1}{e}$ beam radius at the target is calculated to be 0.66 cm). For the smallest glint shown (0.1 mm radius), the irradiance at the receiver is always dominated by the diffuse portion of the target. Consequently the curve labelled 0.1 mm is practically identical to that for a diffuse target alone. (Note the change of scale on the ordinate between Figures 2

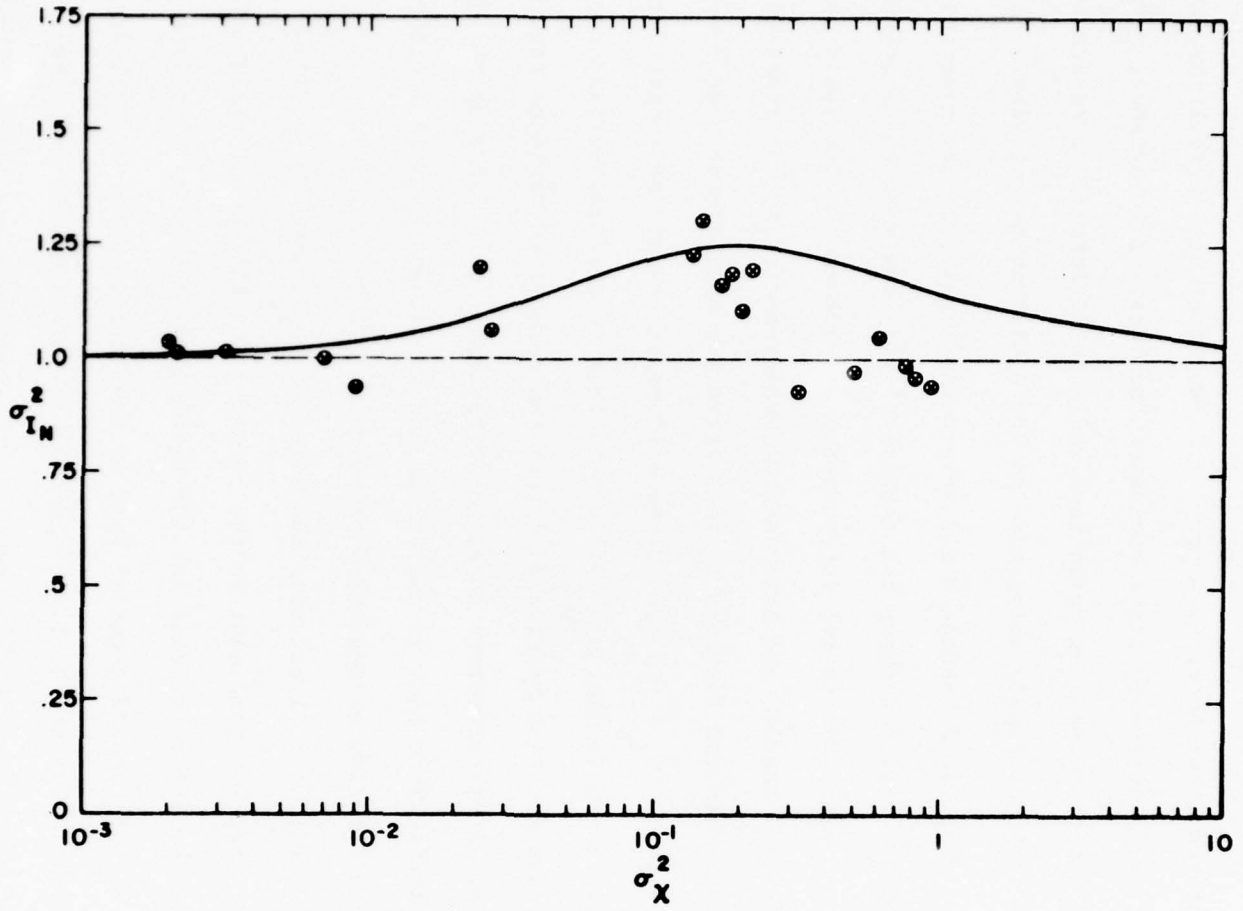

Figure 2. Normalized variance of irradiance vs log amplitude variance for a diffuse target illuminated by a coherent source over a 500 meter path. Solid line is the theoretical curve and ⊕ represent experimental data.

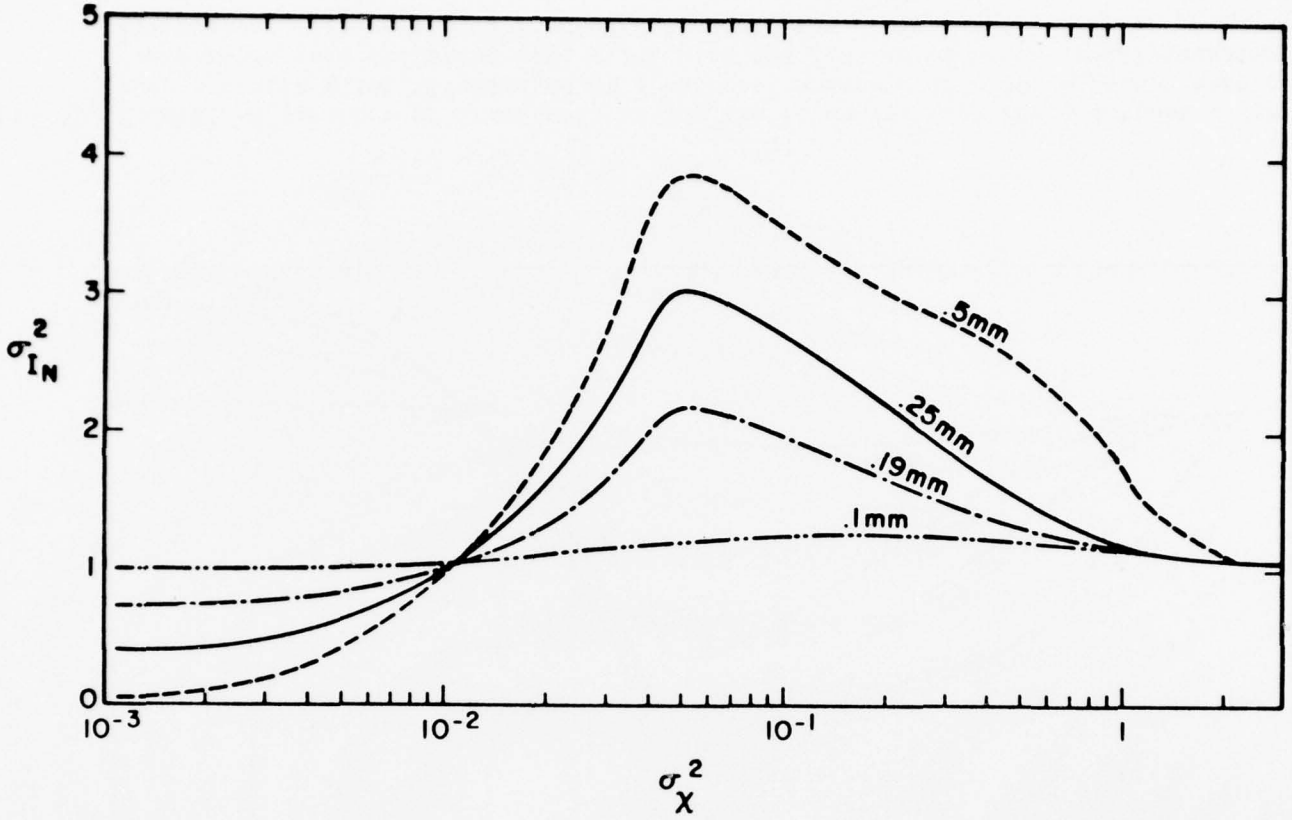

Figure 3. Normalized variance of irradiance vs log amplitude variance for a diffuse target with a single glint illuminated by a coherent source over a 500 m path. Each curve corresponds to a different size glint with the 1/e radius of the model gaussian glint given. The glint is located 1 cm off the optical axis.

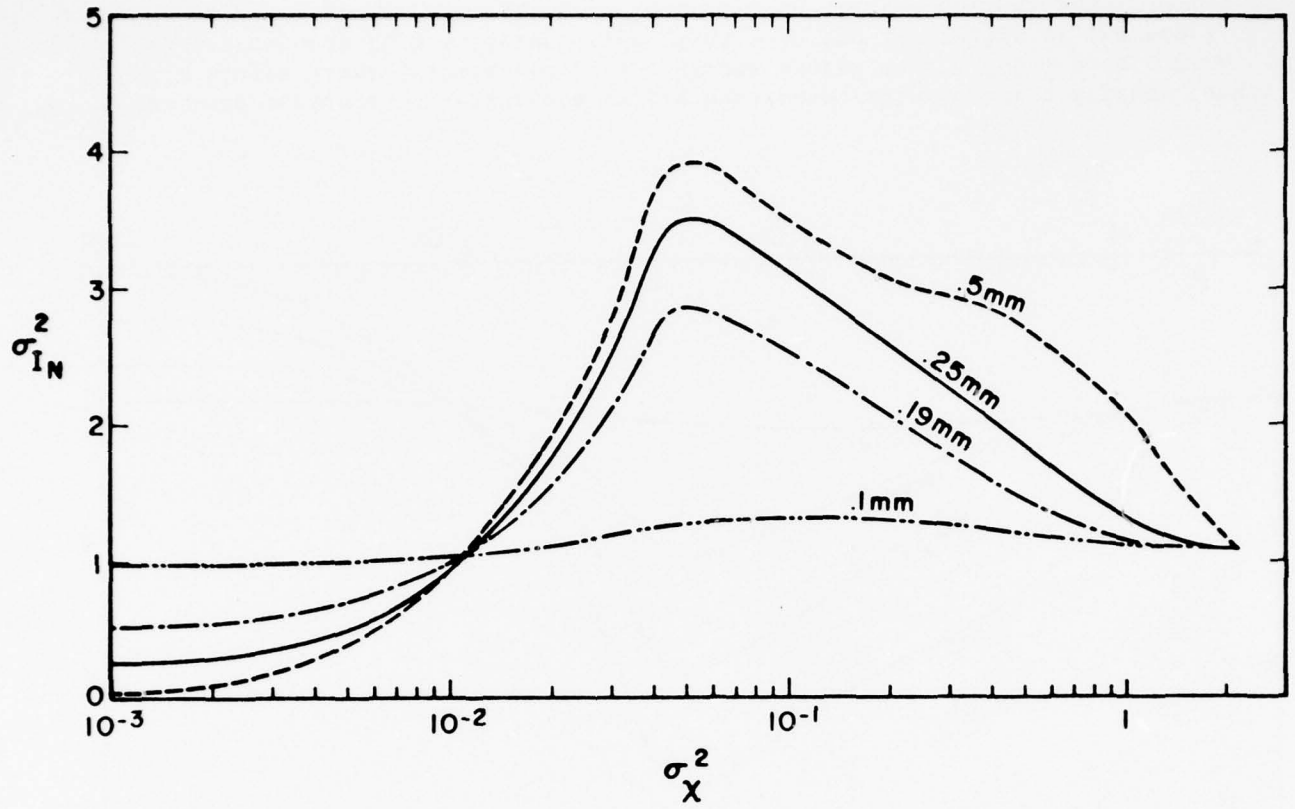

Figure 4. Normalized variance of irradiance vs log amplitude variance for a diffuse target with a single glint illuminated by a coherent source over a 500 m path. Each curve corresponds to a different size glint with the 1/3 radius of the model gaussian glint given. The glint is located 0.5 cm off the optical axis.

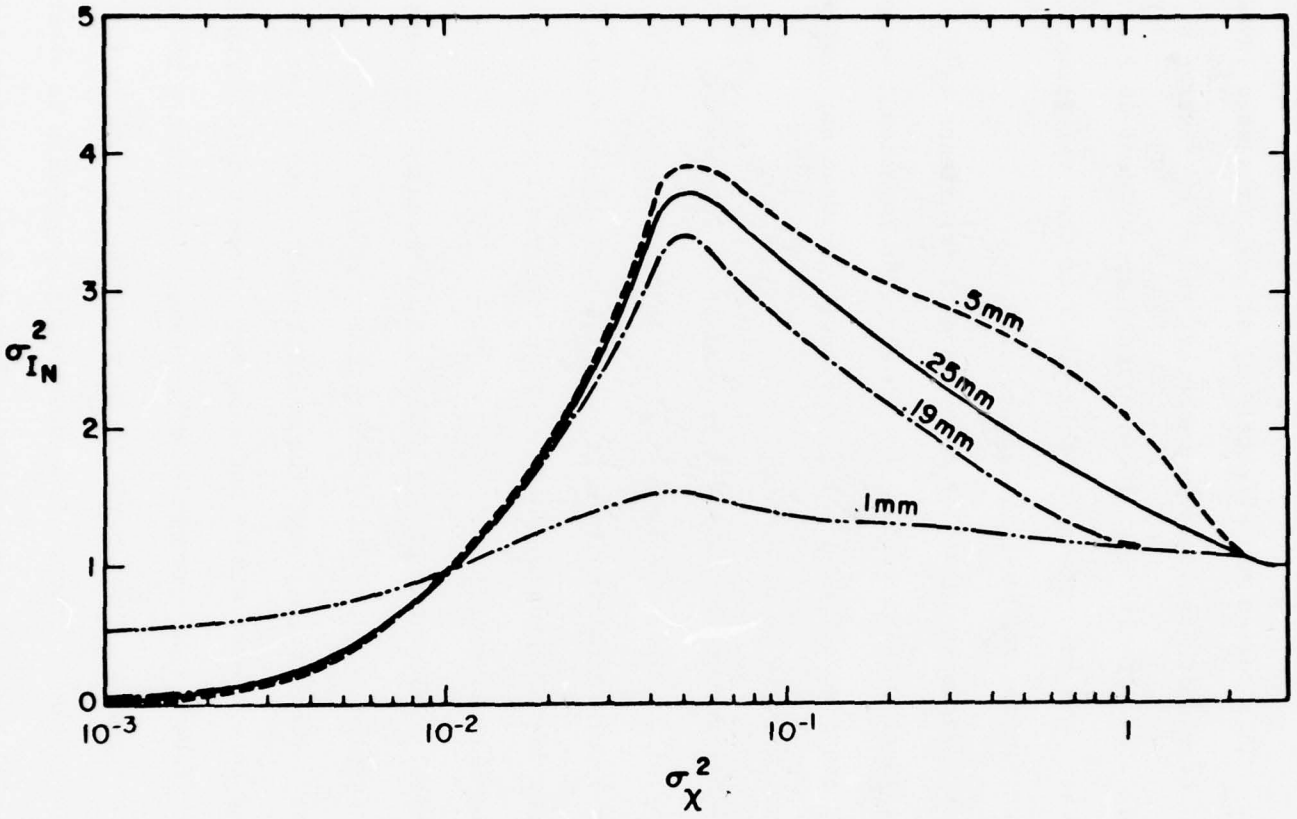

Figure 5. Normalized variance of irradiance vs log amplitude variance for a diffuse target with a single glint illuminated by a coherent source over a 500 m path. Each curve corresponds to a different size glint with the 1/e radius of the model gaussian glint given. The glint is located on the optical axis.

and 3.) As the size of the glint increases, however, the glint term becomes important. This causes two effects: 1) at low turbulence levels, $\sigma_{I_N}^2$ is reduced from unity as would be expected, and 2) $\sigma_{I_N}^2$ peaks up to 3.8 at moderate turbulence levels. These effects are evident in Figures 4 and 5 also, where the only change from Figure 3 is that the glint is located 0.5 cm off axis, and on-axis respectively.

Figure 6 shows the normalized variance of irradiance vs σ_χ^2 for a specular feature of 0.19 mm radius, for three glint locations; on axis, 0.5 cm off axis and 1 cm off axis. This curve will be used for comparison with experimental results in Section IV.

One final feature of interest is evident in Figures 3-5. That is, the tendency of $\sigma_{I_N}^2$ for the largest glint (0.5 mm radius) to "hang up" at a value near 3 before falling to unity at high turbulence levels. This will be discussed in the Appendix where a simplified model is suggested for the large normalized variance.

Numerical evaluations of the analytical expressions derived in the multiple glint case and the partially coherent source case have not been completed. With current techniques, the multiple glint case takes impractically long to evaluate and is not expected to contribute anything fundamentally different than the simple glint case. With regard to the partially coherent source, there seems to be something missing in the analytical understanding of the diffuse scattering that leads to substantial differences between theory and experiment. This case is, consequently, not well understood.

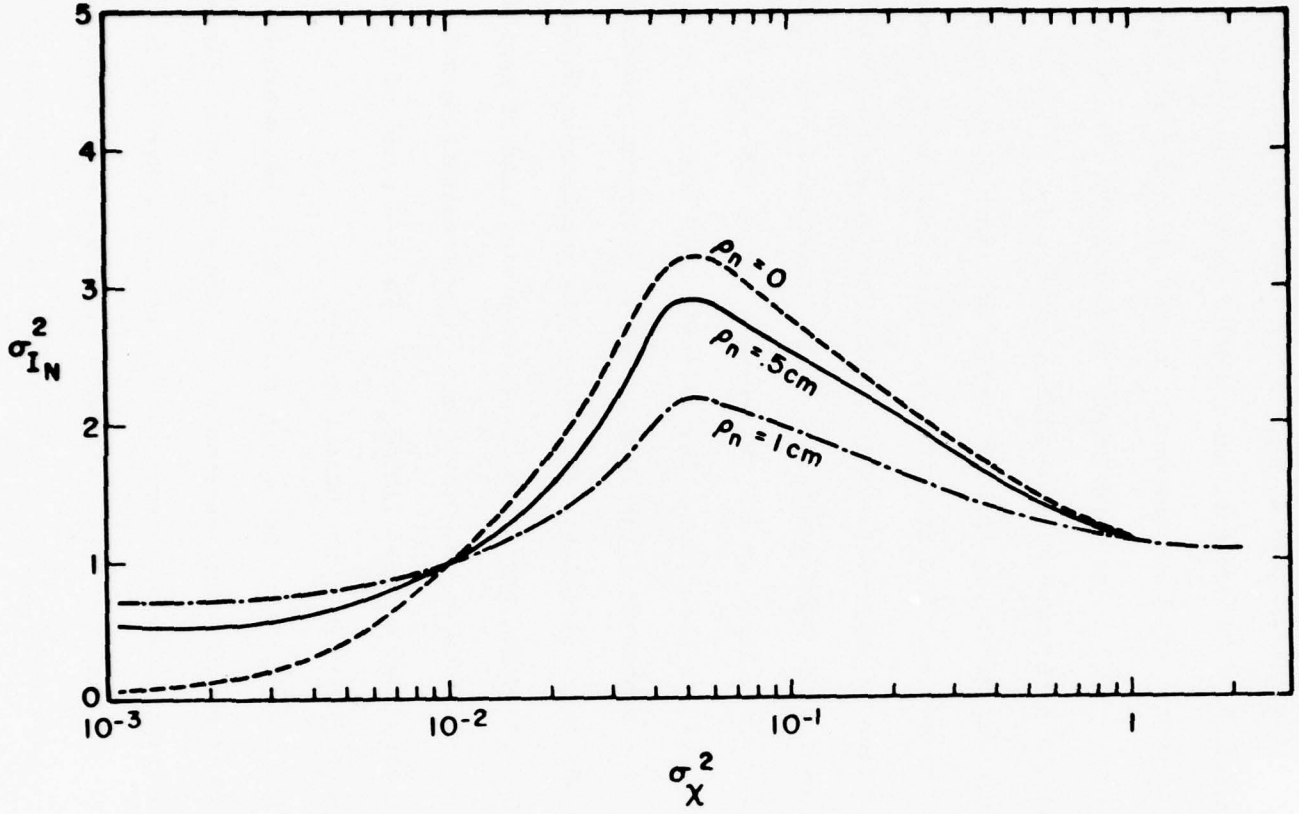

Figure 6. Normalized variance of irradiance vs log amplitude variance for a diffuse target with a single glint illuminated by a coherent source over a 500 m path. The curves are for a model gaussian glint with a 1/e radius of 0.19 mm located on axis, 0.5 cm off axis, and 1 cm off axis.

IV. Experimental Results

A. Introduction

An exprimental program to verify the theory presented in Section II has been conducted. In concept, the experiments were designed to investigate two separate effects; one due to target glint and one due to reduced source coherence. The experimental measurements were made using the facilities and instrumentation described previously.

A Coherent Radiation Model 52 Argon ion laser operating at 488 nm is used as the source. The laser has an output power on the order of 1 watt and contains an intra-cavity etalon that can be used to select a single longitudinal mode when desired. In the transmitter, the laser light is amplitude modulated at 100 kHz using a Morvue PEM-e photo-elastic modulator and a calcite polarizer. The off-axis beam from the polarizer is blocked and the scattered light is detected by a silicon photodiode to provide a 100 kHz local oscillator for use in the synchronous demodulators. The on-axis beam is passed through a convex focussing lens, a spatial filter, and a 7.5 cm diameter objective lens. The resultant beam is steered to the target by a large flat mirror. The 1/e point of the intensity profile is 1.35 cm at the output mirror.

The receiver contains two detectors mounted such that measurements can be made at various detector separations. Each detector consists of an S-20 photomultiplier tube isolated from excess background light by a 10 nm optical bandpass filter, and field of view limiting apertures. The output of the photomultiplier tube feeds an operational amplifier and the resulting signal is passed through a bandpass filter to the synchronous demodulator. The demodulator output is low-pass filtered

and then recorded on a Hewlett-Packard Model HP-3960 fm tape recorder for subsequent processing.

B. Target Glint

The target used in this portion of the experiment was designed to provide a specular feature or "glint" on a diffuse reflecting surface. As in previous work the diffuse surface consisted of Scotchlite (3M Sprint Marking paper). Substantial thought was given to the implementation of the "glint" portion of the target. The eventual decision to use a flat mirror for the majority of the experimental work was based upon the following reasoning:

A "real" glint consists of a specular reflection from a convex curved surface. Experimentally then, our glint should consist of such a surface as opposed to e.g., a retroreflector. Additionally, for this experiment, we wanted the glint to be such that the field strength at the receiver contained comparable contributions from both the glint and from the diffuse surface. Otherwise one or the other component would dominate the statistics. In order to satisfy these two conditions, the required radius of curvature for the convex specular surface glint was so large that a flat mirror provided the practical equivalent.

In order to compare the experimental data with the analytical predictions, we needed to compare our analytical model of a glint with the flat mirror actually used. The analytical model was essentially that of a flat mirror with a gaussian reflectance distribution. In order to compare this with the experimental glint (a flat mirror with a uniform reflectance distribution) the 1/e point of the reflectance was chosen to give the same on-axis mean intensity as that expected from the actual

glint used. Using this as a basis, we obtained good agreement between analysis and experiment.

The variance results are illustrated in Figures 7 and 8. Figure 7 shows the normalized variance of irradiance vs log amplitude variance for a 0.5 mm diameter glint (the analytical model is a flat glint with a gaussian reflectance distribution with a 1/e radius of 0.19 mm). Experimental points are shown as well as the three analytical curves of Figure 6. The curves correspond to a glint located on axis, 0.5 cm off axis and 1 cm off axis. These three curves are shown to illustrate the potential variability of the data with respect to pointing the transmitted beam at the glint and maintaining the pointing throughout the experiment. Note in particular that normalized variances as high as 2.4 were measured in this experiment.

Figure 8 shows experimental measurements and analytical curves for a 4.76 mm diameter, 537 mm radius of curvature spherical glint (modeled by a 0.144 mm 1/e radius gaussian glint). Note again the agreement and in particular the measurement of normalized variances on the order of 1.5.

In addition to variance measurement, the receiver was designed to measure the covariance of irradiance. Selected covariance curves are shown in Figures 9-12.

Figure 9 shows the behavior of the covariance of irradiance as a function of the "strength" of the glint, with the turbulence level constant. (By glint strength we mean the magnitude of the mean irradiance at the receiver which, for a flat glint, is directly proportional to the size of the glint at the target.) As can be seen in the figure, for a

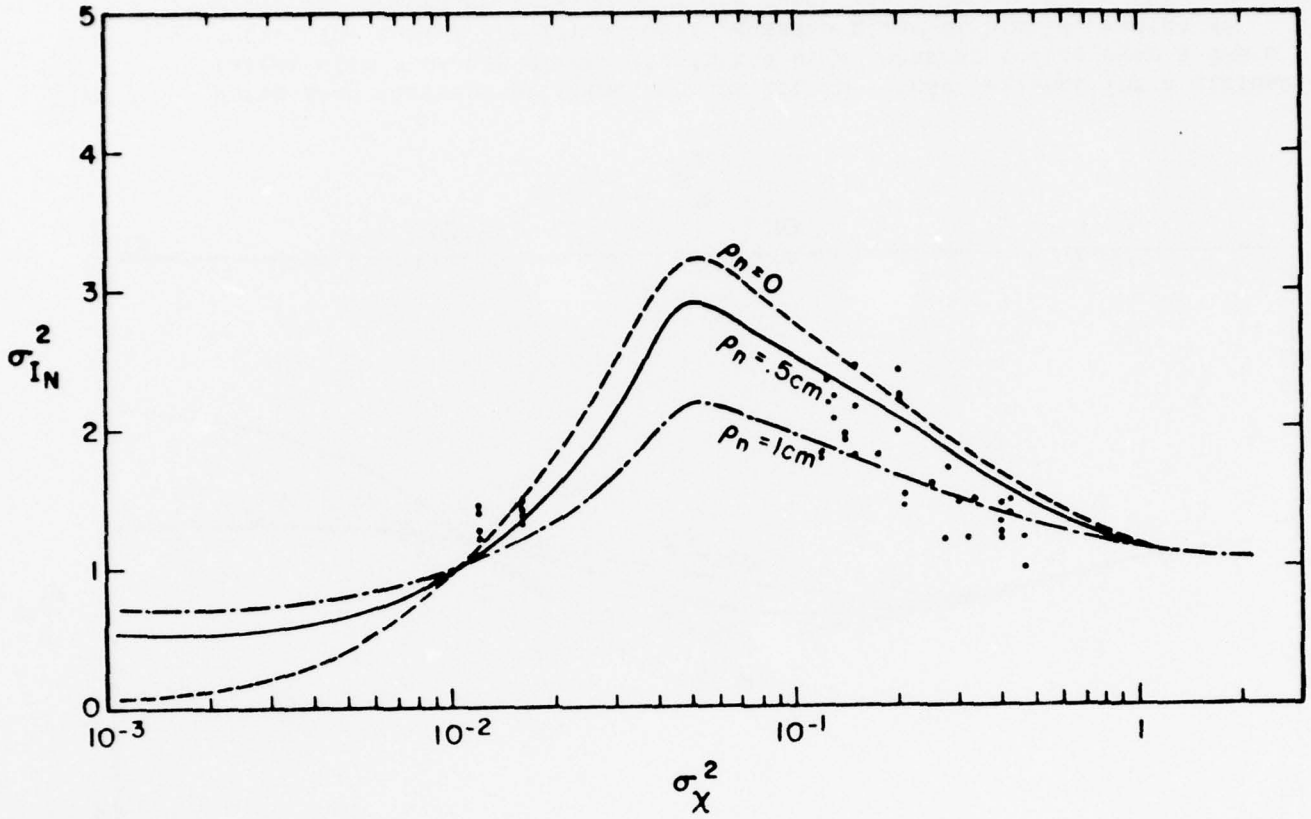

Figure 7. Normalized variance of irradiance vs log amplitude variance for a diffuse target with a single glint illuminated by a coherent source over a 500 m path. The curves are for a model gaussian glint with a 1/e radius of 0.19 mm located on axis, 0.5 cm off axis, and 1 cm off axis. Experimental points are indicated on the figure.

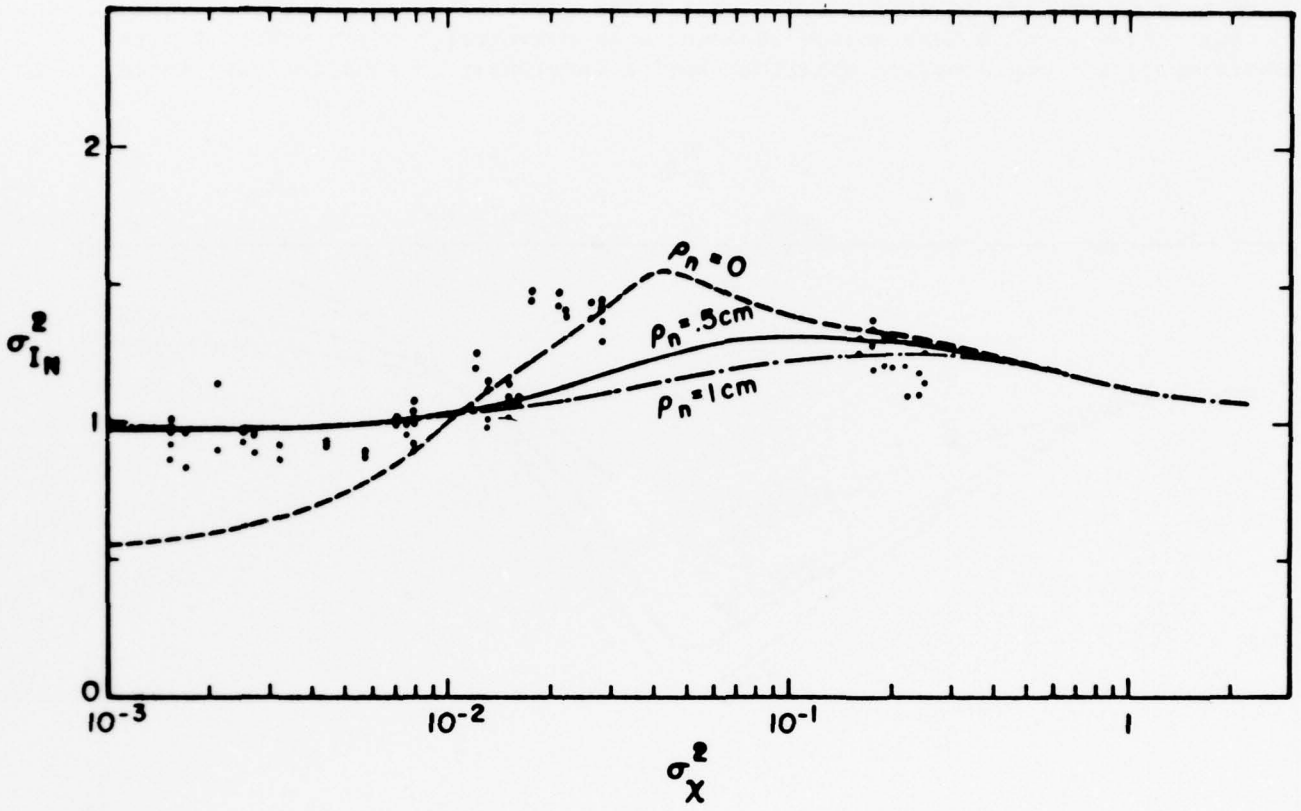

Figure 8. Normalized variance of irradiance vs log amplitude variance for a diffuse target with a single glint illuminated by a coherent source over a 500 m path. The curves are for a model gaussian glint with a 1/e radius of 0.144 mm located on axis, 0.5 cm off axis, and 1 cm off axis. Experimental points are indicated on the figure.

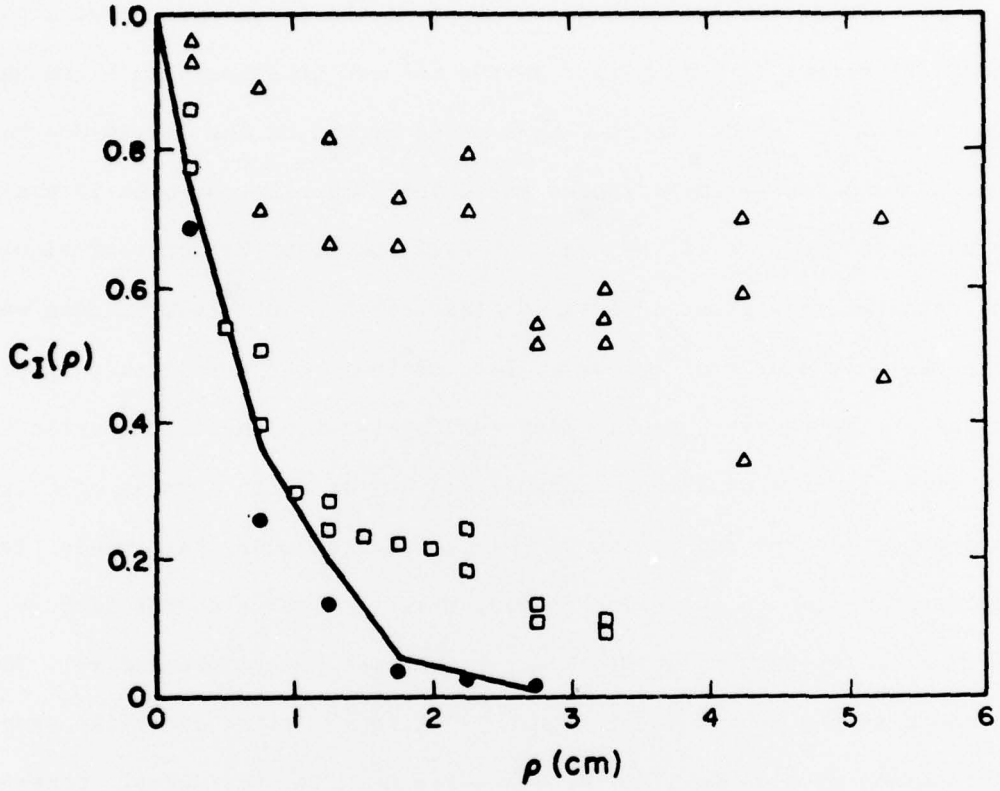

Figure 9. Covariance of irradiance vs separation (ρ) as a function of glint strength for a fixed turbulence level. Solid line - no glint (diffuse target only), solid circles - spherical glint, open squares - 0.48 mm diameter flat glint, open triangles - 1.00 mm diameter flat glint. Path length = 500 meters, $\sigma_\chi^2 = 0.85$.

fixed separation, the covariance increases with glint strength.

Figure 10 shows, for a fixed glint, the narrowing of the covariance with increasing turbulence. Note, however, the "tails" on the covariance curves. These are examined more carefully in the next two figures, where the effect is more evident.

To better understand the shape of the covariance curves, consider the effect of beam wander in the focused gaussian beam illuminating the target.[12] As the incident beam moves around on the target due to beam wander, the illumination of the glint (which in our case is small compared to the size of the beam) changes and from the point of view of the receiver, the glint appears to flash off and on. Thus if beam wander were the only source of intensity fluctuations, the irradiance distribution at the receiver would change uniformly with the illumination of the glint and the covariance curve would be flat with a value of unity, independent of the separation. Under conditions where beam wander is important and where the glint appears bright relative to the diffuse portion of the target, we might expect a broad covariance curve. This is shown in the top curve of Figure 11 where the glint is a flat specular surface of 2.38 mm diameter and where D/ρ_o is near unity. Consequently, with $D/\rho_o = 1$, beam wander is important and we see a broad covariance curve. The lower curve is for $D/\rho_o = 0.2$ with approximately the same log amplitude variance ($\sigma_\chi^2 \approx 0.025$).

This same effect is illustrated in Figure 12. Under conditions where the effect of both wander and scintillations are evident in the covariance curve, the covariance will appear to saturate at a value that

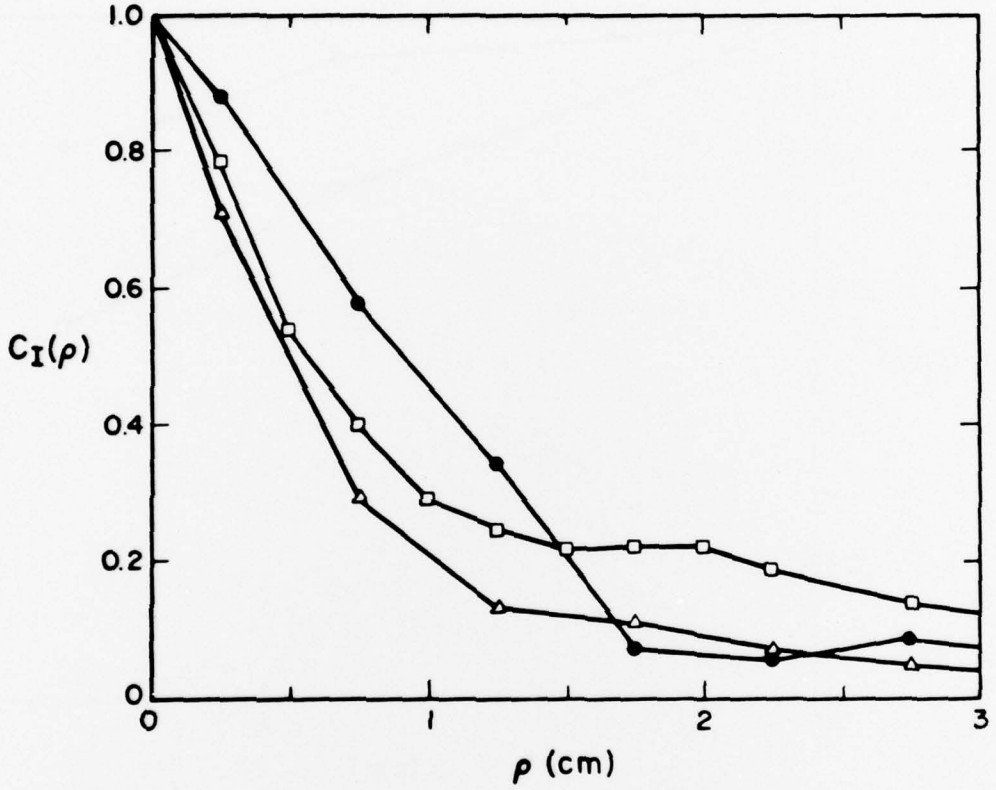

Figure 10. Covariance of irradiance vs separation (ρ) for a 0.48 mm diameter flat glint.

Solid circles - $\sigma_\chi^2 = 0.0014$

Open squares - $\sigma_\chi^2 = 0.015$

Open triangles - $\sigma_\chi^2 = 0.16$

Path length = 500 m

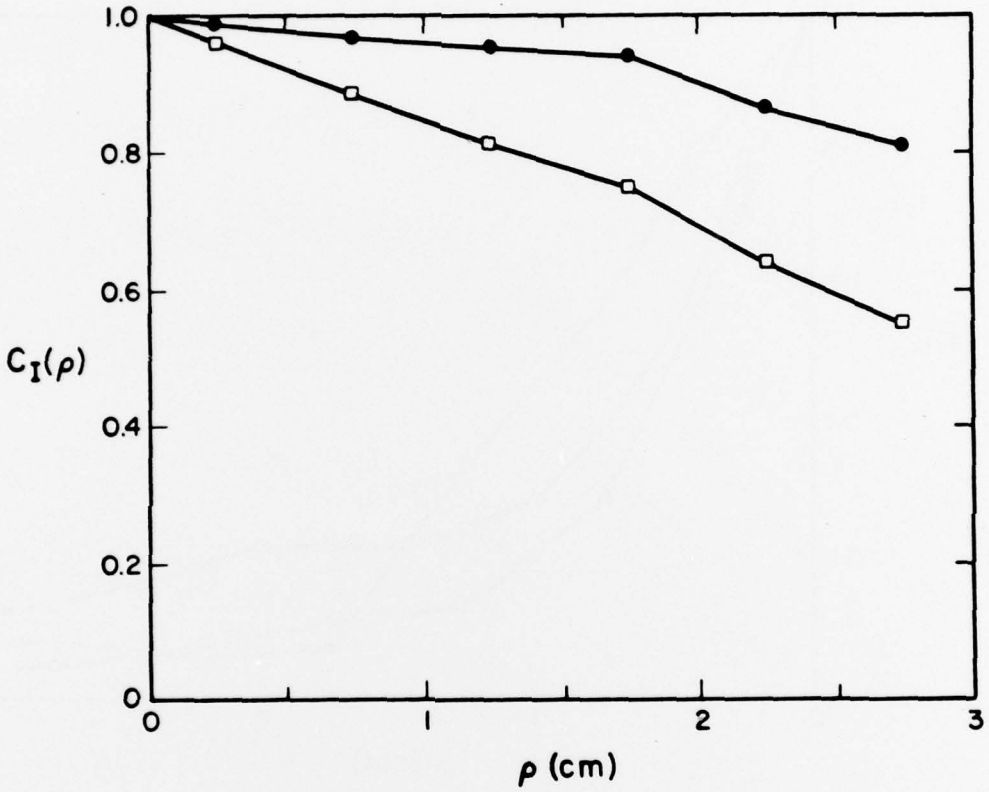

Figure 11. Covariance of irradiance vs separation (ρ) for a 2.38 m diameter flat glint and fixed turbulence level.

Solid Circles - path length = 1500 m, $D/\rho_o = 1.0$

Open Squares - path length = 500 m, $D/\rho_o = 0.19$

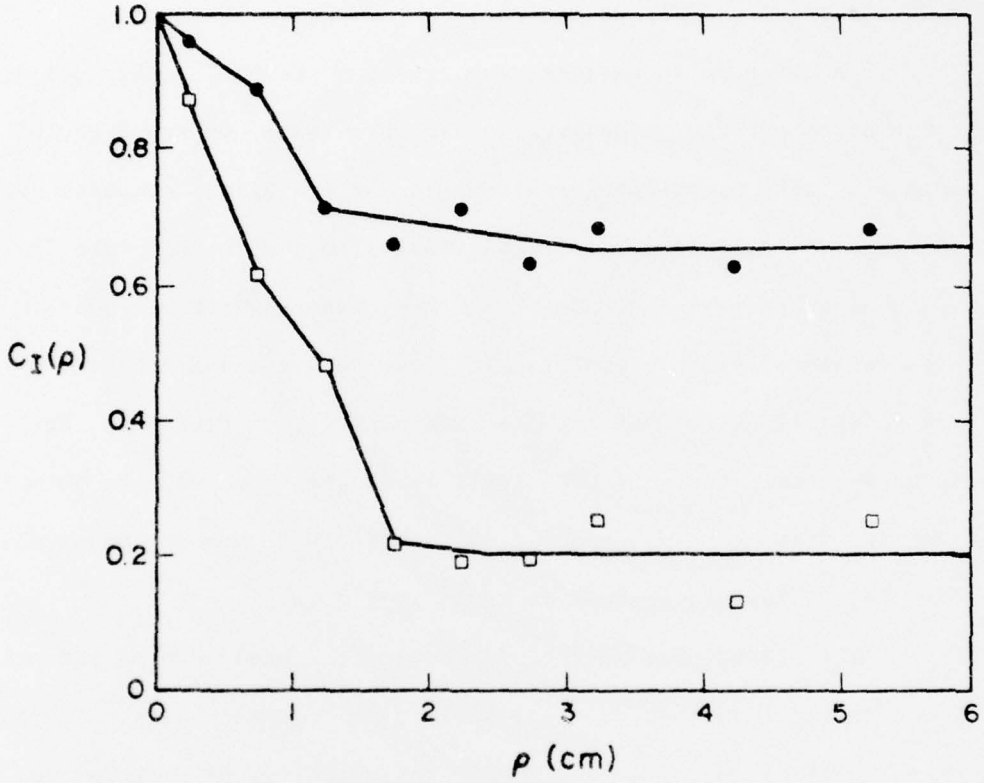

Figure 12. Covariance of irradiance vs separation (ρ).
Solid circles - 2.38 mm diameter flat glint,
$D/\rho_o = 0.35$
$\sigma_\chi^2 = 0.08$
Open squares - 1.00 mm diameter flat glint,
$D/\rho_o = 0.41$
$\sigma_\chi^2 = 0.10$

is proportional to the strength of the glint. This is evident in Figure 12 where the covariance saturates at a higher value for the strongest glint. These covariance curves have not been compared with analytical results due to the complexity of the numerical evaluation of the covariance expressions.

C. Partially Coherent Source

In order to investigate the effect of temporal coherence on the statistics of speckle propagation in turbulence, we repeated the experiments using a completely diffuse target (no glint) composed of scotchlite, and allowed multiple longitudinal modes to oscillate in the argon-ion laser source. This was then compared with previous results obtained using a completely diffuse target and a coherent source (single longitudinal mode) as shown, e.g., in Figure 2. We found unexpectedly that for the partially coherent source, the normalized variance of irradiance was reduced substantially from unity under all conditions. A typical example is shown in Figure 13.

This result was unexpected because the bandwidth of the multimode source was less than or equal to 10^{10} Hz, corresponding to a coherence length of approximately 3 cm. Analytically, we expected no change (less than one percent) in the normalized variance of irradiance for these conditions. The same confusion exists in the absence of turbulence. That is, for zero turbulence, we expect that for the bandwidth given above, the normalized variance of irradiance will be 0.999 for a diffuse surface. When we perform an experiment in the laboratory, over short path lengths such that turbulence may be neglected, we measured normalized variances on the order of 0.3. This was found to

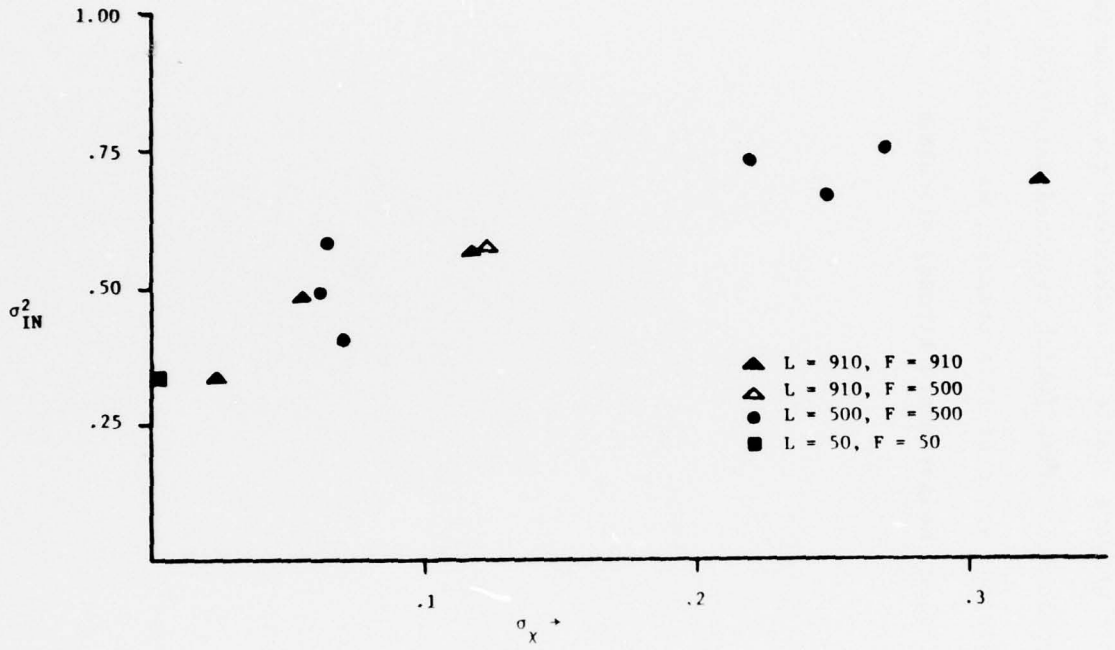

Figure 13. Normalized variance of irradiance vs log amplitude standard deviation for a diffuse target illuminated by a partially coherent source.

be true with scotchlite targets, and also for a variety of other targets simulating a diffuse surface.

Since we were unable to understand the mechanism for the change in speckle statistics (which appeared unrelated to turbulence effects) within the scope of this program, we concentrated our efforts on the target glint measurements already discussed.

V. Discussion

This program has led to several interesting results that include:

- The normalized variance of the irradiance scattered from a target containing a specular feature, and illuminated by a coherent source over a turbulent atmospheric path, may reach a value on the order of 3 (see Appendix for physical model). This corresponds to fluctuations that are much larger than for a diffuse target (normalized variance on the order of unity) and will have a substantial impact on optical systems operating in this geometry.
- The normalized variance of the irradiance scattered from a diffuse target illuminated by a source with reduced temporal coherence is substantially less than when a coherent source is used, and in addition, substantially less than would be expected theoretically. This experimental result appears to be independent of atmospheric effects and is primarily a source target interaction. This result is not well understood and bears further investigation.

Both of these results are significant in the sense that optical systems operating in the presence of atmospheric turbulence, e.g. COAT systems, coherent radar systems, etc., must operate in the presence of these effects. A continuation of the investigation of speckle propagation in the presence of turbulence will lead to improved system

design and analysis, and to improved system performance. Finally a knowledge of the speckle propagation statistics is necessary not only for the design of active optical systems, but for use in understanding countermeasures against these systems.

References

1. M. H. Lee, J. F. Holmes, and J. R. Kerr, J. Opt. Soc. Am. 66, 1164 (1976).

2. J. C. Leader, J. Opt. Soc. Am. 67, 1376 (1977).

3. J. L. Bufton, R. S. Iyer, and L. S. Taylor, Appl. Opt. 16, 2408 (1977).

4. R. F. Lutomirski, H. T. Yura, Appl. Opt. 10, 1652 (1971).

5. H. T. Yura, Appl. Opt. 11, 1399 (1972).

6. H. M. Pedersen, Optica Acta 22, 523 (1975).

7. R. F. Lutomirski, R. E. Warren, Appl. Opt. 14, 840 (1975).

8. "Laser Speckle and Related Phenomena," Edited by J. C. Dainty (Springer-Verlag, New York, 1975).

9. N. George, A. Jain, Appl. Physics. 4, 201 (1974).

10. D. L. Fried, Appl. Opt. 10, 721 (1971).

11. J. R. Kerr, et al., "Propagation of Multiwavelength Laser Radiation Through Atmospheric Turbulence," RADC-TR-77-18, January 1977, A036503.

12. J. R. Dunphy, J. R. Kerr, Appl. Opt. 16, 1345 (1977).

APPENDIX

A simple physical picture of the enhanced normalized variance from a single glint illuminated by a coherent source over an atmospheric path is suggested in this appendix. Consider a bright glint so that the diffuse portion of the target can be neglected. Assume that the effects of turbulence on the illuminating beam and on the reflected beam are independent. Then, from the point of view of the receiver, the glint may be considered as a source whose magnitude is modulated by the scintillations and angle-of-arrival fluctuations of the illuminating beam. Then the magnitude of the source may be modeled by a random variable, X_S, that is directly related to the irradiance of the illuminating beam at the target. The effect of the turbulence on the return path may be modeled as a random variable, X_R. Then the random variable X that represents the irradiance at the receiver, is the product of X_S and X_R, and the normalized variance of X is:

$$\sigma_{X_N}^2 = \frac{\langle X^2 \rangle - \langle X \rangle^2}{\langle X \rangle^2} = \frac{\langle X^2 \rangle}{\langle X \rangle^2} - 1$$

$$= \frac{\langle X_R^2 \; X_S^2 \rangle}{\langle X_R X_S \rangle^2} - 1$$

$$= \frac{\langle X_R^2 \rangle}{\langle X_R \rangle^2} \; \frac{\langle X_S^2 \rangle}{\langle X_S \rangle^2} - 1$$

Now consider the saturated case where the normalized variance of X_R (and X_S) is unity, i.e.

$$\sigma_{R_N}^2 = \frac{\langle X_R^2 \rangle}{\langle X_R \rangle^2} - 1 = 1,$$

MISSION
of
Rome Air Development Center

RADC plans and conducts research, exploratory and advanced development programs in command, control, and communications (C^3) activities, and in the C^3 areas of information sciences and intelligence. The principal technical mission areas are communications, electromagnetic guidance and control, surveillance of ground and aerospace objects, intelligence data collection and handling, information system technology, ionospheric propagation, solid state sciences, microwave physics and electronic reliability, maintainability and compatibility.